Authors' discussion of the comments **bg_2020-312-RC1**

The authors would like to thank Tarek EI-Madany for his helpful comments, which helped us to resolve some ambiguities in the manuscript.

To address the comments in the document *bg_2020-312-RC1*, the authors first copy the exact comment by the reviewer, add numbers to order each comment and make cross-referencing easier, and format in grey and Italic. The answers given by the authors are in black after each comment. In the end of the document, a list of References that support the answers was added.

Major comments

1. *The manuscript entitled "Estimating immediate post-fire carbon fluxes using the eddy-covariance technique" presents a unique data set of carbon-, water-, and energy fluxes measurements 43 days after a wildfire in Portugal. The ecosystem is/was a Maritime Pine with some Eucalyptus stands inside which were mainly burned and only the trunks of the trees remained. The authors explain broadly their data quality control scheme how data were filtered, selected and gap filled. Based on the data they represent cumulative fluxes of NEE GPP and Reco. Additionally, they focus based on one event on the interactions of dew and ashes with respect to carbon dioxide fluxes.Overall the manuscript is well written, but it could need some polishing on the figures as well on the text where sometimes method parts are in the results and discussion parts are in the results. I think this should be cleaned up. Overall, the manuscript is worth to publish especially because we don't have many studies presenting data from ecosystems shortly after a fire disturbance and its recovery. My main concern with the manuscript is that the authors interpret a lot into the eddy covariance data without thaving the right measurements to back it up. See my comments for details. Further, I think the u*-threshold estimation and removal of data with low u* values is nothing to debate about as the eddy covariance technique is not working under those conditions and this must be accounted for in the data processing. For further details see the attached pdf:*

   I would highly recommend a standardized data processing for the gap filling and flux partitioning. The REddyProc (Wutzler et al., 2018) package is easy to use and has all needed functions to do the u-threshold estimation, subsequent gap-filling, and finally the flux partitioning of NEE into Reco and GPP. I think the argument that in this specific case the standardized methods are not working does not hold. In this context I would like to question the QC scheme used here. All fluxes between QC 1 and QC 8 (based on the Foken 1-9 system) are used but here we are already quite far from the assumptions which allow us to apply the eddy covariance technique. I would suggest to go for QC 1-6 to maintain reliable data.*

The authors are surprised by the main statement of the reviewer, that below a u_*-threshold, e.g. 0.28 m s^{-1} (Wutzler et al., 2018) the eddy-covariance method cannot be applied anymore. This would mean that fundamental works on turbulence in the near surface layer, see e.g. Businger et al. (1971) Fig. 8, would have to be revised and all universal functions, especially in the stable range, would be faulty, because in the opinion of the reviewer, the eddy-covariance method can no longer be applied under these conditions. Rather, the pioneers of atmospheric turbulence and the eddy-covariance method have investigated similarity relations that clearly describe the existence of a well-developed turbulence (Wyngaard et al., 1971;Panofsky and Dutton, 1984;Monin and Obukhov, 1954). These have been used to detect a developed turbulence for which the eddy-covariance method can be applied (Foken and Wichura, 1996;Vickers and Mahrt, 1997;Foken et al., 2017).

It is true, however, that by using a u_*-threshold one can be sure that the measurements are not influenced by intermittency, decoupling, gravity waves, low level jets etc. and that no further investigations are necessary. For large measurement programs such as ICOS with central data processing, such a method makes sense, since models can be used in addition to the classical gap-filling methods. However, the present study was not created in the context of such a program, but is a process study, where it is important to include in the study as much original data as possible with developed turbulence and to limit the gap-filling to a necessary minimum because of the reported difficulties to parameterize the equations used for gap-filing. Fig. 1 shows that at a u_* threshold of 0.28 m s^{-1} 37 % data can still be excluded. Together with the 10% of gap-filled data (see Supplement Figure S8), almost half of all data would have to be replaced by parameterized data. This is certainly possible for long-term studies, but not for a process study. This would mainly exclude unstable and stable measurements showing particularly high or low fluxes compared to simple model assumptions (Fig. 2). This would also mean that all weak wind situations below about 2 m s^{-1} are not considered (Fig. 3). The authors therefore decided not to perform the data processing according to a routine method, but to use all possibilities offered by the relevant publications (Foken et al., 2004;Foken et al., 2012a;Foken et al., 2012b;Mauder et al., 2013). Critical is that these are many self-quotes, but the work has been developed together with renowned scientists from this field, such as L. Mahrt, R. Leuning and M. Aubinet.

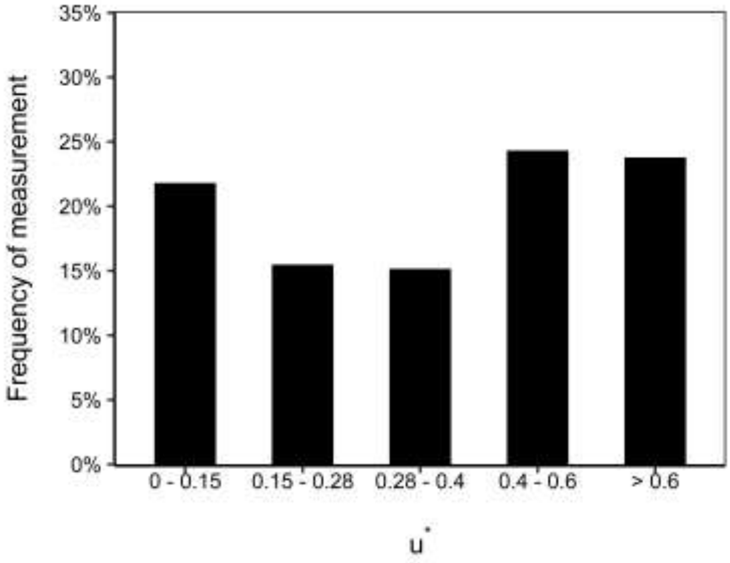

Fig. 1: Frequency of the friction velocity

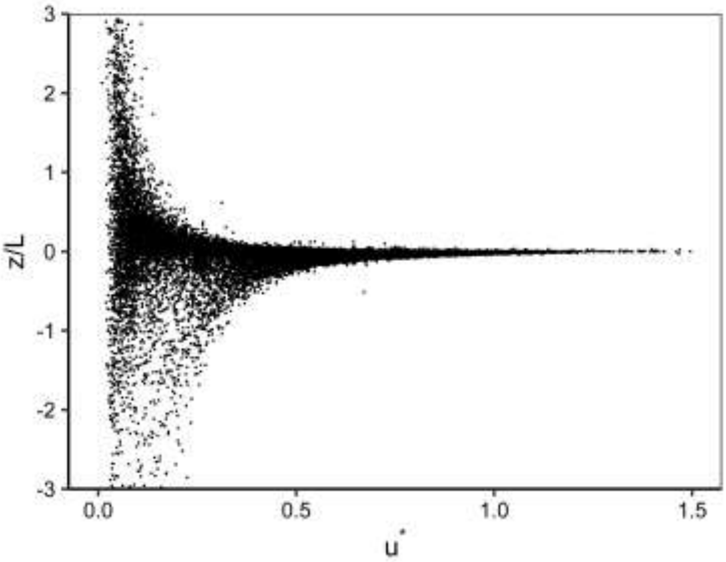

Fig. 2: Friction velocity as a function of stability (z/L, z: height, L: Obukhov length)

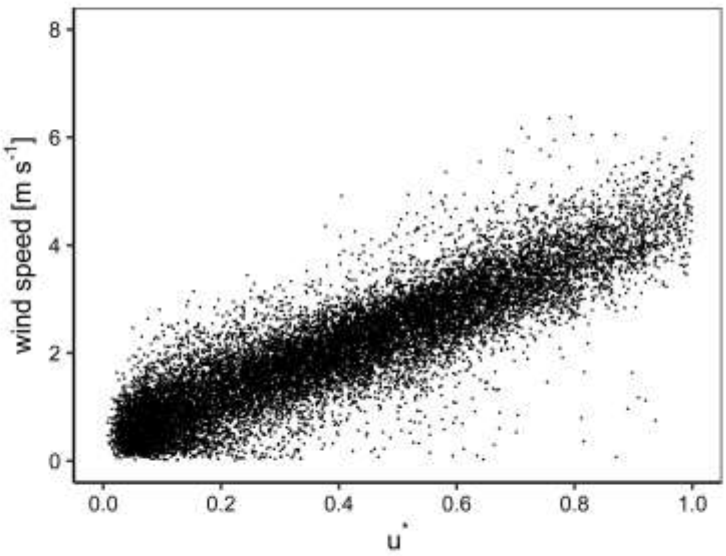

Fig. 3: Dependence of the friction velocity on the wind speed

The answers to the following major and minor comments of the reviewer must be considered in the light of these statements, so that details are not repeated again. It is sometimes difficult to separate the results and discussion sections for reasons of readability and understanding. The authors will therefore change the headings:

R**esults → Results and specific discussions;**

Discussion → Overall discussion

2. *.Within the manuscript for different analysis different QC schemes are used which is very confusing. Sometimes wind sectors are removed then again, they are not. In one instance QC 1-6 is used in another QC 1-9 this is confusing for the reader because it jumps back and forth.*

The authors do not use two different QC schemes. We only use QC 1-6 for gap-filling (Supplement S7), otherwise Q 1-8 (Supplement S8) if we carefully check the causes of the bad flags. **The authors will check the text again to see if this is clear enough.**

The background is the recommendation that for basic investigations such as the determination of the functions for gap-filling only classes 1-3, if possible 1-6 should be used (see Foken et al., 2012b, p. 117-118). This option is only available for individual data processing.

3. *The uptake in burned area after the fire is either a measurement artefact or it comes from vegetation that is still taking up carbon. Maybe arising from imperfect footprint estimates? Or a too tall canopy height which will reduce the footprint size and thus suggest that footprints are smaller than they are in real (minor comments below)? Which in turn would reduce the number of footprints having 80% of Maritime Pine contribution. In the east there is the eucalyptus patch close to the tower. Not much is mentioned about it but it seems to be the second most important wind direction and thus potentially influencing the measurements?*

The authors actually already referred these hypotheses on lines 522-525: "Possibly, this immediate post-fire photosynthetic activity originated from various patches of pines with scorched crowns to the northeast and south of the EC tower and/or from re-sprouting eucalypts, in particular the 4 individual trees near the tower and/or the patch to the east of it."

Elaborating further on this matter, the authors would like to clarify that the patches of scorched pine crowns were present between 22 September 2017 and 03 January 2018 but no longer on 05 March 2018 (as the pine needles had dropped to the forest floor). This can be seen on the ortho-photomaps included at the bottom of this rebuttal. The eucalypt patch to the east of the tower (see Figure 1 in the Manuscript) could be an alternative or complementary source, either through post-fire photosynthetic activity of the scorched crowns (visible – as shadows - on the 22 Semptember2017 ortho-photomap, at least for the closest trees) or through newly emerging sprouts. However, the relevance of this potential eastern source is probably reduced, due to the low frequency of the eastern sector (see Figure 2 of the Manuscript and answer to minor comment 16). The 4 individual eucalypt trees at relatively close distance to the west of the tower, shown in Figure 1 of the Manuscript, could also be an alternative or complementary source. However, all 4 trees suffered complete crown consumption by the fire, as is visible on the 22 September 2017 ortho-photomap, and only showed very reduced recovery three months later, as is evident on the 03 January 2018 ortho-photomap. In resume, the authors believe that the scorched pine patches are the most likely source of the observed carbon assimilation immediately after the fire but we have not measured the photosynthetic activity of scorched pine needles and are also not aware of any previous study on that.

Since the burnt area around the tower mainly consist of maritime pine woodland, a smaller footprint is not expected to reduce the number of footprints with 80% pine

Although the text explicitly refers that the fire burnt a total area of 12.5 km^2 (line 65), the map can indeed be somewhat misleading as to the extent of the burnt area around the study site. The minimal distance to the unburned area was 1.1 km in the W-NW sector. This is outside the footprint.

It is possible that the text does not make it clear enough that the forest fire was a large-scale fire, i.e. the areas adjacent to the area under investigation were also completely burned down. While in the case of pine trees only single charred tree trunks remain, eucalyptus trees still have completely dried leaves, but without any assimilation or respiration function. **The authors will clarify this again in the text.**

The authors also investigated the question of possible artifacts. We have selected two periods with nearly equal energy input for which > 80% of the footprint is determined by pine (Fig. 10) and eucalyptus (Fig. S12), respectively. There were no significant differences in the CO_2 fluxes, so that a "not exact" footprint does not lead to artifacts.

The question of eucalyptus trees in the east is examined in detail in section 3.1.1. The sonic anemometer type CSAT3 was set up in such a way that the impermissible backward flow is largely identical with the flow through the trees. As Fig. 6 shows, this leads to a reduction of the data quality. In some cases, the data quality is so bad due to mechanical turbulence that the data were replaced. Looking at the investigations in sections 3.1.1 and 3.3.3 it becomes clear that these trees only have an influence on the mechanical turbulence and not on the CO_2 flow.

4. *The data set associated to this discussion paper is only containing daily data for NEE, GPP and Reco. But most analysis are based on half hourly data. I guess it would be nice to also have those data available in the dataset. But this depends on the journal / editors decision.*

As far as the authors know, in long-term studies (e.g. Keenan et al., 2014) are used as common units g C m^{-2} d^{-1} or g C m^{-2} yr^{-1}. Thus, a user of the data no longer needs to convert µmol m^{-2} s^{-1}. Since we are still exploring further the half hourly data set for further studies, we have opted for only making available the daily data set, at least for the time being. At the same time, lines 456-457 explicitly state that "Other data can be requested by email to bruna.oliveira@ua.pt."

Minor comments

1. *L42-43 not fully clear if the ecosystem is still a source on an annual basis or considering the totally emitted carbon vs. the total carbon sequestered by the ecosystem during the following 10 years.*

The reference Dore *et al.* (2008) is included in Table S1. In summary, the authors only measured the ecosystem fluxes 10-years after a stand-replacing wildfire. Even though the authors write "Ten years after the fire, the burned site was still a source of CO_2 to the atmosphere (…)" they do not present data that support a constant behavior during the 10 years. Hence, the ecosystem might have behaved as a C sink in previous years.

Following the comment of the reviewer, the text in the Manuscript was slightly adapted from

"Furthermore, these effects can be long lasting, as well illustrated by Dore et al. (2008), finding that a 10-year old burnt site was still a carbon source."

to

"Furthermore, these effects can be long lasting, as illustrated by Dore et al. (2008), finding that a Pinus ponderosa forest was a carbon source 10-years after a stand-replacing wildfire (Supplementary Material Table 1)."

2. *L57 maybe adding a city or village would make it easier to find.*

Following the suggestion of the reviewer, the village "Vila de Rei" was added to the text. Since the installation is still in operation and the equipment is without fencing or other type of protection, the authors do not want to disclose the exact location of the study area to avoid vandalism, as experienced in the past by the team.

3. *L78-79 How can a median value have a range (4.5 -6.7m)?*

The original sentence was:

"*Median height and diameter-at-breast-height of the burnt pine trees ranged from 4.6 to 6.7 m and from 2.5 to 4.3 cm, respectively.*"

Following the comment of the reviewer, the sentence was updated to:

"Median height and diameter-at-breast-height of the burnt pine trees in each of the 5 plots selected for fire severity assessment ranged from 4.6 to 6.7 m and from 2.5 to 4.3 cm, respectively."

to make more clear that 4.5 – 6.7 is not the median tree height in the footprint area and refers only to the fire severity assessment plots.

4. *Figure 1 Include the slope angle map from the supplementary figure 1 and also add a map with the footprint climatology. Also add the points for the fire severity sampling into the map.*

Following the suggestion of the reviewer, the slope angle map will be transferred from the supplementary material to the manuscript and the fire severity assessment points will be added to one map in the Supplementary material.

The authors do not have a Footprint climatology (Amiro, 1998;Göckede et al., 2008), because the present study is not a long-term study but a process study. We do not see the cumulative flux as the main result of the present paper. The reported wind climatology and footprint distribution allow sufficient conclusions about the footprint climatology.

5. *L100 Based on what was the zero-plane displacement set to 3.8m and the canopy height to 8m if the median height only goes up to 6.7 m? This seems wrong.*

The authors agree that the canopy height of 8 m may lead to some confusion, given the information provided on tree height in the 5 fire severity assessment points in L78-79. As mentioned in a previous comment, **the text in L78-79 was reformulated** to:

"Median height and diameter-at-breast-height of the burnt pine trees in each of the 5 plots selected for fire severity assessment ranged from 4.6 to 6.7 m and from 2.5 to 4.3 cm, respectively."

In L98-99 the authors wrote:

"The – standing - pine trunks in the immediate surroundings of the tower were approximately 8 m high, and this was used as "canopy" height in all calculations, together with a zero-plane displacement of 3.8 m."

Hence, the authors believe that with the reformulation in L78-79 the information on canopy height is now more clear.

The determination of zero-plane displacement proves to be extremely complicated in a heterogeneous area, especially if there are only single roughness elements (charred trees). We followed the recommendation in this regard and evaluated only the highest roughness elements (Leclerc and Foken, 2014, p. 34). An exact determination would only be possible by parallel profile and flux measurements (Foken, 2017). Since areas with burned pine trees and eucalyptus in the CO_2 fluxes do not differ significantly, the error on the footprint determination should be small.

6. *Table 1 I assume the wind vector components at 20Hz were likewise sampled with the CSAT 3 correct? If so please insert that for "Sensor" instead of sonic anemometer.*

The authors updated Table 1 to make more clear that the sensor CSAT3 was used to determine the wind vector (3 components) and sonic temperature.

7. *Table 1 The EC5 Sensors are not mentioned in the table but should be included.*

Following the suggestion of the reviewer, the EC5 sensors were added to Table 1:

Height	Parameter	Sensor	Manufacturer	Remarks
(…)				
-2.5; -7.5; -10; -20; -30 cm	Soil temperature and volumetric water content	GS3 sensor linked to a Em50 data logger	GS3 sensor linked to a Em50 data logger	1.5 m from tower; 0.02 Hz data
-2.5; -7.5 cm	Soil volumetric water content	EC5 sensors linked to Em50 data loggers	DECAGON Devices	3 EC5 at -2.5 cm and 1 EC5 at -7.5 cm in each of 5 points along the footprint area
-2.5 cm	Soil temperature and volumetric water content	GS3 sensors linked to Em50 data loggers	DECAGON Devices	1 GS3 in 5 points along the footprint area

and the corresponding text in L104-109 was clarified, also considering minor comments 14 and 15 by the reviewer:

"In addition to the soil moisture/temperature station immediately next to the tower listed in Table 1, five soil moisture/temperature stations were installed along the above-mentioned transect. Each station comprised 4 EC5 soil moisture sensors and 1 GS3 soil moisture/temperature. Of the sensors in each of the 5 stations, 1 EC5 was near the roots of a burnt pine tree, 1 EC5 was near the roots of a reprouter shrub (Pterospartum tridentatum), 1 EC5 at -2.5 cm and 1 EC5 at -7.5 cm in the inter-patch (clearing), and 1 GS3 at -2.5 cm in the inter-path. In this study, only the data from the soil moisture sensors installed at -2.5 cm at the inter-patches were used."

8. *L129 – 131 What percentage of the half hourly footprint contribution were used to determine the contribution of the pine trees (e.g. 80%, 90%, 95%)?*

The distribution of pine trees in the Footprint sector is shown in Figure 4. For the process studies (non-cumulative flux) only data with Footprint > 80% were used. Note: Footprint models determine the Footprint area (effect level) relatively accurately, but the exact local allocation is often insufficient due to the influence of crosswind fluctuations (Markkanen et al., 2009, 2010).

9. *L138 the supplementary material is not ordered as they appear in the text. This should be Figure S2. Please change accordingly throughout the manuscript and supplementary material accordingly.*

The authors appreciate that the reviewer pointed this. **The order of the Figures in Manuscript and Supplementary Material will be revised.**

10. *L150-152 The night time estimation is very coarse and might create huge biases especially during the winter period when sunrise and sunset are clearly later and earlier, respectively. I would recommend to use the potential radiation to estimate day- and nighttime. This is for example included in the REddyProc package that can also take care of the gap-filling as well as flux partitioning including u*-threshold estimation.*

The gap-filling of the data was done according to the exact sunrise and sunset times (Supplement Figure S8). A significantly tighter time frame was chosen for the processing of the parameterization of the data for gap-filling. Thus, data with significant sensible heat flows were excluded in order to keep the additive WPL correction, which is in the order of magnitude of the flux, as low as possible (Webb et al., 1980, Fig. 1).

The sentence:

L278 *"Respiration fluxes were determined using only the measurements from 10 pm to 04 am UTC, with more than 80% of the footprint area from the Maritime Pine stands, and with quality flags 1-6."*

will be reformulated to:

"Respiration fluxes were determined using only the measurements from 10 pm to 04 am UTC **to reduce the influence of the additive WPL correction (Webb et al., 1980)***, with more than 80% of the footprint area from the Maritime Pine stands, and with quality flags 1-6."*

11. *L157 I think "initial slope" is better than "linear slope" given that the function is not linear.*

Following the comment of the reviewer, the text will be updated.

12. *L158-159 I would argue that α and Qc,sat are no constant but variable based on environmental conditions which are not just a function of air temperature but also of vapor pressure deficit (VPD), soil water content (SWC) and status of the vegetation. Qc,sat will increase based on the leaf area index (LAI). Was this procedure done for individual periods or windows e.g. 4 weeks? This would be important to clarify.*

The procedure was done for temperature classes only, and the results are summarized in Table 3. **The authors will include "for temperature classes" in the table.** LAI determination was not yet possible in the first year after the fire (see Supplementary Figures p. 14)

13. *L168-169 what were the upper and lower threshold for the mean vertical wind speed?*

Following the comment of the reviewer, the authors noticed that the 1-minute input files for the wavelet analysis were coordinate rotated. **The authors will change the text accordingly.**

14. *L177 Why was not 10 and 20cm used and instead the average? Further your first sensor is at -2.5 cm so the integral should be from -0.025 to -0.15 (equation 3). From Table one it seems that only the sensors 1.5. to the tower were used but not the whole transect. Is this correct? If so I would suggest to also use the other profiles from the transect to get a better spatially representative average soil heat flux.*

Equation 3 is in line with the references Liebethal and Foken (2007) and Yang and Wang (2008). We have therefore omitted further details. The data of the temperature sensors above 15 cm depth have of course been included in the determination of the storage term (2nd term of the equation). The depth 10 and 20 cm were needed to determine the heat flux at 15 cm depth. The soil sensors along the transect did not measure deeper than 7.5 cm, as now listed in Table 1 and explained in L104 (please see answer to minor comment 7). Data from these sensors was only used to determine the volumetric soil water content classes, as detailed in Section 2.3.5.

15. *L186 not clear what inter-patch means. I assume the sensors from the transect. Please indicate this also in table 1 and in lines 107-108. Which sensors were used for what? It is not consistent because the deeper VWC sensors were also used for estimating the soil heat flux.*

Following this and related comments of the reviewer (minor comments 7 and 14), **the text in L104-109 was updated** to make the experimental setup more clear:

"In addition to the soil moisture/temperature station immediately next to the tower listed in Table 1, five soil moisture/temperature stations were installed along the above-mentioned transect. Each station comprised 4 EC5 soil moisture sensors and 1 GS3 soil moisture/temperature. Of the sensors in each of the 5 stations, 1 EC5 was near the roots of a burnt pine tree, 1 EC5 was near the roots of a reprouter shrub (Pterospartum tridentatum), 1 EC5 at -2.5 cm and 1 EC5 at -7.5 cm in the inter-patch (clearing), and 1 GS3 at -2.5 cm in the inter-path. In this study, only the data from the soil moisture sensors installed at -2.5 cm at the inter-patches were used."

16. *L209 what is the value of q for your data set?*

The value for the q parameter in Equation 5 used in each MAD analysis is referred in the Results section: for the Energy balance closure, q = 0.5 was used (L261); and for the gap-filling of respiration, q= 0.5 was used (L81).

17. *L230-231 If all data from that wind direction (30 – 90 degree) are flagged and removed this should be included in the schemes for data treatment. Also, it would be helpful if Figure 2 would be adjusted in a way that the 30° sectors fit to the bins of figure 6.*

Please see major comment 3: This comparison is not possible. Figure 2 are mean data. Fluxes are based on turbulence data with a significant variation of the cross-wind component, which can be up to ± 45° for the wind direction (see e.g. Foken and Leclerc, 2004, Fig. 7). Besides the roughness influence there is a significant stability influence (Blackadar, 1997). Thus, the data selection was made according to the individual quality classes and not generally according to the mean wind sector.

18. *Figure S8 more details on the individual symbols and numbers could be needed. I think total number of removed data is quite low given all quality criteria mentioned. If I see that correctly there are about 10-15 % of all data missing to their wind direction (30 – 90°), further there are 40 % of data with not enough Maritime Pine coverage in the footprint area. But from Figure S8 it looks like only 1727 data points were removed and gap filled.*

Please see major comment 3 and minor comment 17.

19. *Figure S4 the different grey colors are hard to distinguish. Would be nice to add different symbols to the individual lines. Additionally, this figure shows nicely how wrong a fixed period between 10pm and 4 am is for night time estimates. Even around end of June the sunrise is just around 6am UTC when considering the increase in H and net radiation. The same is true for the nighttime.*

The authors will add symbols to the Figure. For the second part, please see minor comment 10.

20. *L245-248 What about heat storage in the burned trunks of the trees? This is something that is not considered or discussed here. The half hourly fluxes are missing the storage term of heat but this is not discussed. Additionally, the trunks certainly contribute to the sensible heat fluxes and increase the surface area compared to the bare soil. Further it is not clear if these trees are also fully in the field of view of the net radiometer. Especially in the morning at high solar zenith angle the trees will absorb a lot of the short-wave incoming radiation, heat up and contribute to the sensible heat flux. This would happen in the morning and the afternoon. Something for the discussion I guess.*

The present study is not to investigate the closure of the energy balance. For this purpose, all conditions are missing both with regard to instrumentation and necessary additional information (Mauder et al., 2020). For this reason, the figures are not in the article but in the supplement for interested readers. Such inadequacies are the choice of the net-radiometer, the heterogeneity of the surface with soil, ashes, wood residues etc., and also the still standing charred tree trunks (the number is not large, because in Figure 3 you can still see the horizon well). The examination of the energy balance is in the sense of quality control (Foken et al., 2004;Foken et al., 2012b) and a proper execution of the measurements can be assumed with a closure of 80-100 %. The authors do not see the need to complete the text.

21. *Figure S5 The linear equation is very small and hard to read including the r² values. As you did not provide an offset value in the formula I assume you forced the intercept to be 0? Please state that explicitly if it is the case. If the detection limit of 10 W m-2 was used then this should be an absolute value. During nights with wind you might get negative sensible heat fluxes which can be larger than -10 and the same is true for latent heat during those nights just that it will in most cases not be negative. Also mention that there is the confidence interval of the linear fit included as the grey shaded area. The number of points going into the linear relation estimate should also be mentioned.*

The authors will improve the visual quality of the Figures. Due to the reasons for the closure of the energy balance, night time measurements should be excluded from the assessment of the residual, which the authors have done. The authors will not go into this further here, as this is comprehensively stated in review articles and the references cited there (Foken, 2008;Mauder et al., 2020).

22. *L257-259 how do we know that net radiation was underestimated? Due to the tilting? Is there a hysteresis in the net radiation and we do know that there is overestimation in the afternoon and underestimation in the morning caused by the tilting toward SW (L253)? This is not clear at all. This tilting would overestimate the incoming components in the afternoon and underestimate them in the morning which could then lead to the observed pattern. Is that the reasoning? How do we know there is an overestimation in the long wave outgoing? What evidence do we have for that? Many of these thoughts belong in the discussion and not the results I would say.*

It is not the tilting because, as said in the comment, this leads to both over- and under-determination. All net-radiometers that do not measure all 4 radiation components separately have the problem of too low readings (10-20%). This has basically been investigated by Halldin et al. (1992). This is also discussed in the overview papers on energy balance (Foken, 2008). The authors have quoted a paper specifically on the problems of NR-lite (Brotzge and Duchon, 2000) and believe that in Lines 253-257 this is sufficiently stated.

L235: *"Net radiometers, as the one used in this study (Table 1), that do not measure the four up- and down-welling long- and shortwave radiation components separately, are well-known to underestimate net radiation (Kohsiek et al., 2007)."*

23. *L264-270 this is all discussion and no results. And even for the discussion I think this is not really needed. Your manuscript is not about the problems of energy balance closure under post-fire conditions but to characterize ecosystem fluxes. I find this whole hypothetical discussion on where the non-closure is quite distracting from the main objective. And we all know that the energy balance is not closed at any site. With you lack of 10% you are actually closer than most sites around the globe.*

The authors agree with this comment, please see answer to minor comment 22. However, it is important to determine whether the CO_2 flux must be corrected or not.

24. *L273-276 I don't agree at all with statement. I don't see why the development of vegetation is a reason not to use standard gap-filling procedure? There are many grasslands in the Mediterranean or other dry areas which senesce during the summer and regreen during the autumn and winter. It is the same as happening here. And all of these sites in FLUXNET use the standard gap filling and flux partitioning schemes similar to the one used in REddyProc. So this is not a valid reason. The second point is somewhat true because moving windows smear the signal when rapid changes are happening e.g. the re-wetting of the ecosystem after the summer. Still if you are interested in the annual sums which also seems to be a point of the manuscript I would highly suggest to use standard gap-filling and flux partitioning.*

In the authors opinion, it is doubtful whether when can directly compare seasonal patterns in plant activity in a Mediterranean and dryland grasslands with vegetation recovery from wildfire. The present results also demonstrate this, in the sense that they show basically no vegetation activity during the start of the autumn rainfall season as would be expected from a system reviving from summer senescence.

According to Papale (2012) there are different methods to achieve an optimal gap-filling. The method of Wutzler et al. (2018) is one but not the only one. The authors have followed the basics of gap-filling (Falge et al., 2001a, b) to the same extent as it was done in all other papers. The only difference is that we did not use a method with a u_*-criterion. We have explained this extensively in major comment 1. Instead, the authors used the method of Ruppert et al. (2006), in which the comparison to the u_*-method was also made.

It must be added that the fluxes in the present work are very small and that, in addition to the usual processes of assimilation and respiration, the microbial decomposition of ashes also plays a role on which there is little knowledge so far.

25. *L289 E0 "0" must be subscript*

Following the comment of the reviewer, the text was updated.

26. *L300-305 Formula 6 is not fully explained. What is T in this formula? Is it the surface temperature as assumed by the Stefan-Boltzman law? How was this then estimated or is it the air temperature. The reasoning and how this was derived should be explained in the methods and not in the results. I would recommend to move this part to methods section. And at the end of line 305 a point is missing.*

The authors apologize for missing half sentence stating what T in Equation 6 is.

L305 was updated to *"where σ_{SB} is the Stefan-Boltzmann constant and T is the temperature at 11.8m height.* "

This very rough estimation is possible considering error considerations for long wavelength radiation (Gilgen et al., 1994). It is certainly useful to move this to the methods section. However, there are only 4 lines and it could affect the clarity. The authors will decide this after presentation of the other reviews.

27. *3.2.3."Generating the final data set" this part is not consistent with what is written in the methods and what is shown in the schematics. Here night time is defined different as compared to the methods part (L150). Here nothing is mentioned about the filter of wind direction or the footprint filter. This is confusing.*

For time please see minor comment 9. **The authors will change the section title to "3.2.3 Generating the final data set for cumulative fluxes"**. For the process studies, as noted there, for example, higher demands were made on the footprint.

28. *L336 first time that the storage term is mentioned. This should be made clear in the methods part. And it should be mentioned if it was the 1-point storage correction or based from a multiple point vertical profile system.*

Following the reviewer suggestion, **it was added to the Methods (L126) that the software packaged used, TK3, estimates the CO_2 storage flux from one point CO_2 measurements** as suggested by Hollinger et al. (1994).

29. *Figures S9 and S10 it is very hard to associate the events across variable of the plots. First the horizontal zero lines should be included. Secondly the areas with dew should be shaded vertically so the points can be clearly associated and compared across the different variables. To me it looks like we see a flushing of CO2 in the morning that accumulated during the night at the ground. If the 1-point storage correction was used this one will for sure not capture what is happening at the ground. How was the friction velocity during the night? This could also tell a bit about the storage of CO2 at the ground. If the moment of the high CO2 flux goes together with an increase in u* then we can be quite sure that this was rather a flush of CO2 than CO2 originating from instantaneous microbial activity or water flowing into pores and flushing out CO2. Also the argument of the negative sensible heat flux is not very convincing. Dew evaporation needs energy but we must separate the individual processes. As long as we have a negative net radiation and we reached already 100% relative humidity we will observe more dewfall which means a negative latent heat flux (this was actually not shown in figure 8). Only when energy is provided in form of incoming short-wave radiation we can have conditions of evaporation. But then the energy for evaporation is coming from the incoming short-wave radiation which means sensible heat is not increasing fast but slow. The negative sensible heat flux looks to me like an inversion of cold air at the surface was breaking up in the morning and transporting cold air upwards together with the CO2. I think here we are missing many data streams to bring the story together.*

The authors have investigated this case very carefully: Figures S9 and S10 were included in the supplement to show the relevant conditions on the days from September 26 to 29. The discussion of the dew fall can only be seen in Figure 8. The friction velocity at the relevant time was 0.05-0.10 m s^{-1}, so that a dynamic effect can be excluded. Also the assumption of the influence of the storage term is not applicable, because the fluxes were calculated with the wavelet tool (Schaller et al., 2017). The sensible heat flux is a good indicator for the dewfall, because then it is positive, while it is negative for evaporation without additional short wave radiation. The latent heat flux is too small to represent the process well.

The statement that short-wave radiation is necessary for evaporation (evaporation, not transpiration) is wrong. The example shown here can be classified as an oasis effect (Stull, 1988). An impressive example is shown in Foken (2017, Fig. 1.14). Evaporation occurs when moisture is present, a water vapor pressure gradient exists, and turbulence is present. If no short wave radiation is present, the energy can also be provided by long wave cooling (negative sensible heat flux) or the ground heat flux.

The authors will improve the visual quality of the Figures.

30. *Figure S12 and S13 here it seems very clear that the burned area is more heterogeneous as expected. Else the fluxes would be more homogeneous and not scatter so much. This indicates that there are patches which take up carbon. Maybe a better representation would be a plot of midday NEE or CO2 flux vs wind direction. I think this would make it clearer and highlight the differences between the burned and the other areas and maybe also give you more trust in the differences you see. Maybe I would even do it for every month/ season but this is just a suggestion.*

The dry cases Figures 10 (pine) and S12 (eucalyptus), which were selected for the respective surface with > 80% in the footprint regarding all 30-minute fluxes, must be compared. No significant fluctuations can be detected. The magnitude of the fluctuations is typical for the influence of turbulence, low cloud cover etc. Figure S13 shows a case after/with precipitation (also footprint > 80% for pine). Here the fluctuations are naturally larger, whereby surely different humidification and cloudiness play a role. After the wildfire there were no unburnt areas in the close vicinity of the tower and it was only in April 2018 that the green areas became visible (Fig. 04).

See also answer to major comment 3.

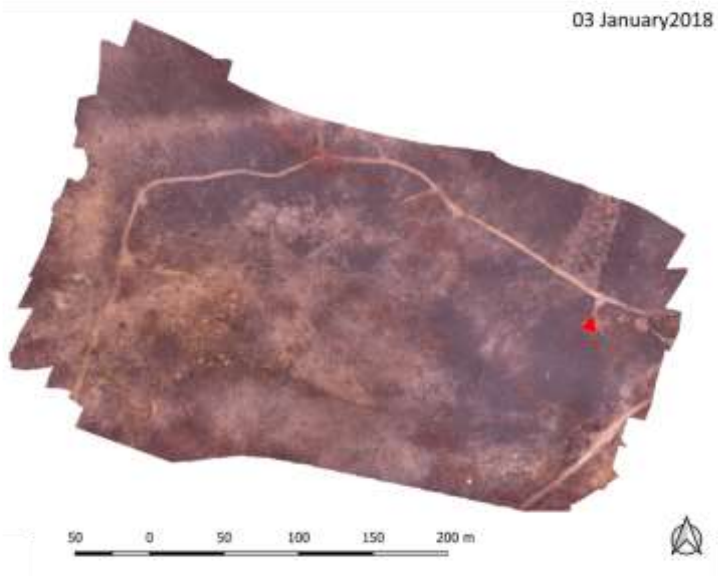
03 January2018
50
0
50
100
150
200 m

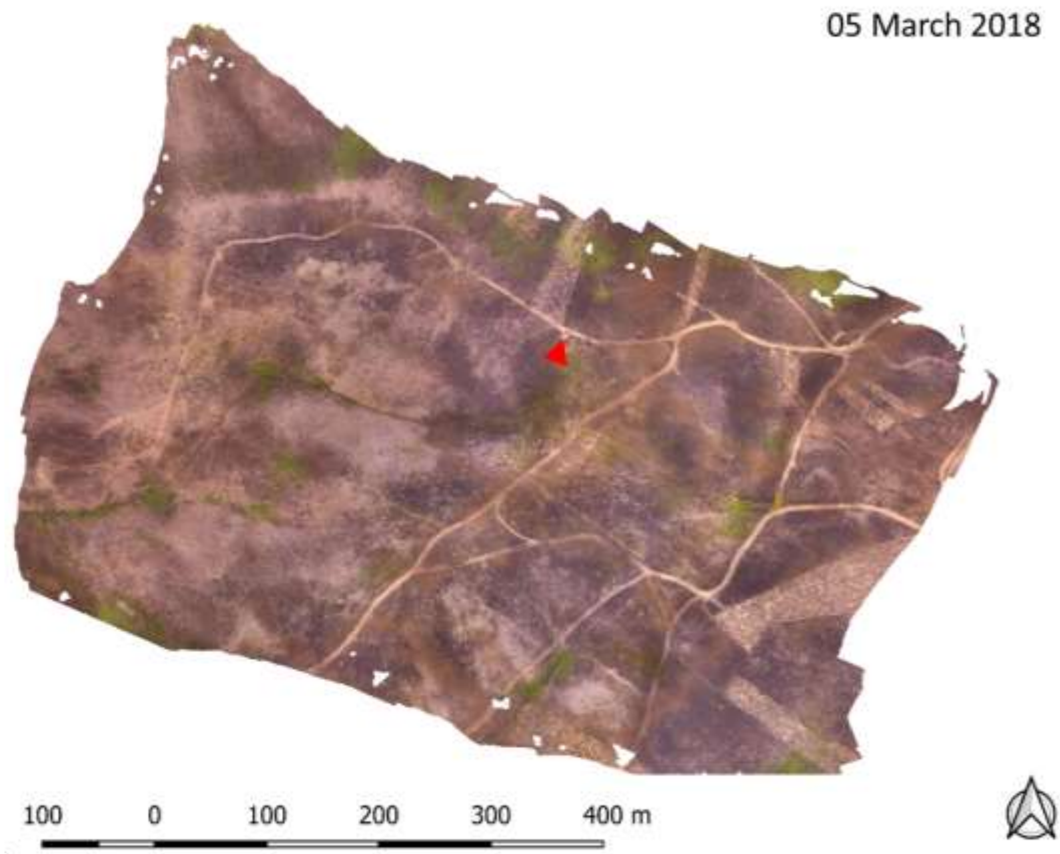
05 March 2018
100
0
100
200
300
400 m

Fig. 04: UAV-based ortho-photomaps of the burnt area to the west of the EC tower (marked as a red triangle) on 22 September 2017 and 03 January 2018, and of the burnt area surrounding the EC tower on 05 March 2018.

References

Amiro, B. D.: Footprint climatologies for evapotranspiration in a boreal catchment, Agric. For. Meteorol., 90, 195-201, doi, 1998.

Blackadar, A. K.: Turbulence and Diffusion in the Atmosphere, Springer, Berlin, Heidelberg, 185 pp., doi, 1997.

Brotzge, J. A., and Duchon, C. E.: A Field Comparison among a Domeless Net Radiometer, Two Four-Component Net Radiometers, and a Domed Net Radiometer, J. Atm. Oceanic Techn., 17, 1569-1582, doi: 10.1175/1520-0426(2000)017<1569:AFCAAD>2.0.CO;2, 2000.

Businger, J. A., Wyngaard, J. C., Izumi, Y., and Bradley, E. F.: Flux-profile relationships in the atmospheric surface layer, J. Atmos. Sci., 28, 181-189, doi: 10.1175/1520-0469(1971)028<0181:FPRITA>2.0.CO;2, 1971.

Falge, E., Baldocchi, D., Olson, R., Anthoni, P., Aubinet, M., Bernhofer, C., Burba, G., Ceulemans, R., Clement, R., Dolman, H., Granier, A., Gross, P., Grunwald, T., Hollinger, D., Jensen, N. O., Katul, G., Keronen, P., Kowalski, A., Lai, C. T., Law, B. E., Meyers, T., Moncrieff, H., Moors, E., Munger, J. W., Pilegaard, K., Rannik, U., Rebmann, C., Suyker, A., Tenhunen, J., Tu, K., Verma, S., Vesala, T., Wilson, K., and Wofsy, S.: Gap filling strategies for defensible annual sums of net ecosystem exchange, Agric. For. Meteorol., 107, 43-69, doi, 2001a.

Falge, E., Baldocchi, D., Olson, R., Anthoni, P., Aubinet, M., Bernhofer, C., Burba, G., Ceulemans, R., Clement, R., Dolman, H., Granier, A., Gross, P., Grunwald, T., Hollinger, D., Jensen, N. O., Katul, G., Keronen, P., Kowalski, A., Lai, C. T., Law, B. E., Meyers, T., Moncrieff, H., Moors, E., Munger, J. W., Pilegaard, K., Rannik, U., Rebmann, C., Suyker, A., Tenhunen, J., Tu, K., Verma, S., Vesala, T., Wilson, K., and Wofsy, S.: Gap filling strategies for long term energy flux data sets, Agric. For. Meteorol., 107, 71-77, doi, 2001b.

Foken, T., and Wichura, B.: Tools for quality assessment of surface-based flux measurements, Agric. For. Meteorol., 78, 83-105, doi: 10.1016/0168-1923(95)02248-1, 1996.

Foken, T., Göckede, M., Mauder, M., Mahrt, L., Amiro, B. D., and Munger, J. W.: Post-field data quality control, in: Handbook of Micrometeorology: A Guide for Surface Flux Measurement and Analysis, edited by: Lee, X., Massman, W. J., and Law, B., Kluwer, Dordrecht, 181-208, doi, 2004.

Foken, T., and Leclerc, M. Y.: Methods and limitations in validation of footprint models, Agric. For. Meteorol., 127, 223-234, doi, 2004.

Foken, T.: The energy balance closure problem – An overview, Ecolog. Appl., 18, 1351-1367, doi: 10.1890/06-0922.1, 2008.

Foken, T., Aubinet, M., and Leuning, R.: The eddy-covarianced method, in: Eddy Covariance: A Practical Guide to Measurement and Data Analysis, edited by: Aubinet, M., Vesala, T., and Papale, D., Springer, Dordrecht, Heidelberg, London, New York, 1-19, doi: 10.1007/978-94-007-2351-1_1, 2012a.

Foken, T., Leuning, R., Oncley, S. P., Mauder, M., and Aubinet, M.: Corrections and data quality in: Eddy Covariance: A Practical Guide to Measurement and Data Analysis, edited by: Aubinet, M., Vesala, T., and Papale, D., Springer, Dordrecht, Heidelberg, London, New York, 85-131, doi: 10.1007/978-94-007-2351-1_4, 2012b.

Foken, T.: Micrometeorology, 2nd ed., Springer, Berlin, Heidelberg, 362 pp., doi: 10.1007/978-3-642-25440-6, 2017.

Foken, T., Göckede, M., Lüers, J., Siebicke, L., Rebmann, C., Ruppert, J., and Thomas, C. K.: Development of flux data quality tools, in: Energy and Matter Fluxes of a Spruce Forest Ecosystem, Ecological Studies Vol. 229, edited by: Foken, T., Springer, Cham, 277-308, doi: 10.1007/978-3-319-49389-3_12, 2017.

Gilgen, H., Whitlock, C. H., Koch, F., Müller, G., Ohmura, A., Steiger, D., and Wheeler, R.: Technical plan for BSRN data management, WRMC, Techn. Rep., 1, 56 pp, doi, 1994.

Göckede, M., Foken, T., Aubinet, M., Aurela, M., Banza, J., Bernhofer, C., Bonnefond, J.-M., Brunet, Y., Carrara, A., Clement, R., Dellwik, E., Elbers, J. A., Eugster, W., Fuhrer, J., Granier, A., Grünwald, T., Heinesch, B., Janssens, I. A., Knohl, A., Koeble, R., Laurila, T., Longdoz, B., Manca, G., Marek, M., Markkanen, T., Mateus, J., Matteucci, G., Mauder, M., Migliavacca, M., Minerbi, S., Moncrieff, J. B., Montagnani, L., Moors, E., Ourcival, J.-M., Papale, D., Pereira, J., Pilegaard, K., Pita, G., Rambal, S., Rebmann, C., Rodrigues, A., Rotenberg, E., Sanz, M. J., Sedlak, P., Seufert, G., Siebicke, L., Soussana, J. F., Valentini, R., Vesala, T., Verbeeck, H., and Yakir, D.: Quality control of CarboEurope flux data – Part 1: Coupling footprint analyses with flux data quality assessment to evaluate sites in forest ecosystems, Biogeosci., 5, 433-450, doi: 10.5194/bg-5-433-2008, 2008.

Halldin, S., and Lindroth, A.: Errors in net radiometry, comparison and evaluation of six radiometer designs, J. Atm. Oceanic Techn., 9, 762-783, doi, 1992.

Hollinger, D. Y., Kelliher, F. M., Byers, J. N., Hunt, J. E., McSeveny, T. M., and Weir, P. L.: Carbon dioxide exchange between an undisturbed old-growth temperate forest and the atmosphere, Ecology, 75, 134-150, doi, 1994.

Keenan, T. F., Gray, J., Friedl, M. A., Toomey, M., Bohrer, G., Hollinger, D. Y., Munger, J. W., O/'Keefe, J., Schmid, H. P., Wing, I. S., Yang, B., and Richardson, A. D.: Net carbon uptake has increased through warming-induced changes in temperate forest phenology, Nature Clim. Change, 4, 598-604, doi: 10.1038/nclimate2253, 2014.

Leclerc, M. Y., and Foken, T.: Footprints in Micrometeorology and Ecology, Springer, Heidelberg, New York, Dordrecht, London, XIX, 239 pp., doi: 10.1007/978-3-642-54545-0, 2014.

Liebethal, C., and Foken, T.: Evaluation of six parameterization approaches for the ground heat flux, Theor. Appl. Climat., 88, 43-56, doi: 10.1007/s00704-005-0234-0, 2007.

Markkanen, T., Steinfeld, G., Kljun, N., Raasch, S., and Foken, T.: Comparison of conventional Lagrangian stochastic footprint models against LES driven footprint estimates, Atmos. Chem. Phys., 9, 5575-5586, doi: 10.5194/acp-9-5575-2009, 2009.

Markkanen, T., Steinfeld, G., Kljun, N., Raasch, S., and Foken, T.: A numerical case study on footprint model performance under inhomogeneous flow conditions, Meteorol. Z., 19, 539-547, doi, 2010.

Mauder, M., Cuntz, M., Drüe, C., Graf, A., Rebmann, C., Schmid, H. P., Schmidt, M., and Steinbrecher, R.: A strategy for quality and uncertainty assessment of long-term eddy-covariance measurements, Agric. For. Meteorol., 169, 122-135, doi: 10.1016/j.agrformet.2012.09.006, 2013.

Mauder, M., Foken, T., and Cuxart, J.: Surface Energy Balance Closure over Land: A Review, Boundary-Layer Meteorol., online first, doi: 10.1007/s10546-020-00529-6, 2020.

Monin, A. S., and Obukhov, A. M.: Osnovnye zakonomernosti turbulentnogo peremesivanija v prizemnom sloe atmosfery (Basic laws of turbulent mixing in the atmosphere near the ground), Trudy geofiz. inst. AN SSSR, 24 (151), 163-187, doi, 1954.

Panofsky, H. A., and Dutton, J. A.: Atmospheric Turbulence - Models and Methods for Engineering Applications, John Wiley and Sons, New York, 397 pp., doi, 1984.

Papale, D.: Data gap filling, in: Eddy Covariance: A Practical Guide to Measurement and Data Analysis., edited by: Aubinet, M., Vesala, T., and Papale, D., Springer, Dordrecht, Heidelberg, London, New York, 159-172, doi, 2012.

Ruppert, J., Mauder, M., Thomas, C., and Lüers, J.: Innovative gap-filling strategy for annual sums of CO_2 net ecosystem exchange, Agric. For. Meteorol., 138, 5-18, doi: 10.1016/j.agrformet.2006.03.003, 2006.

Schaller, C., Göckede, M., and Foken, T.: Flux calculation of short turbulent events – comparison of three methods, Atmos. Meas. Techn., 10, 869-880, doi: 10.5194/amt-10-869-2017, 2017.

Stull, R. B.: An Introduction to Boundary Layer Meteorology, Kluwer, Dordrecht, 666 pp., doi: 10.1007/978-94-009-3027-8, 1988.

Vickers, D., and Mahrt, L.: Quality control and flux sampling problems for tower and aircraft data, J. Atm. Oceanic Techn., 14, 512-526, doi: 10.1175/1520-0426(1997)014<0512:QCAFSP>2.0.CO;2, 1997.

Webb, E. K., Pearman, G. I., and Leuning, R.: Correction of the flux measurements for density effects due to heat and water vapour transfer, Quart. J. Roy. Meteorol. Soc., 106, 85-100, doi: 10.1002/qj.49710644707, 1980.

Wutzler, T., Lucas-Moffat, A., Migliavacca, M., Knauer, J., Sickel, K., Šigut, L., Menzer, O., and Reichstein, M.: Basic and extensible post-processing of eddy covariance flux data with REddyProc, Biogeosci., 15, 5015-5030, doi: 10.5194/bg-15-5015-2018, 2018.

Wyngaard, J. C., Coté, O. R., and Izumi, Y.: Local free convection, similarity and the budgets of shear stree and heat flux, J. Atmos. Sci., 28, 1171-1182, doi, 1971.

Yang, K., and Wang, J.: A temperature prediction-correction method for estimating surface soil heat flux from soil temperature and moisture data, Sci. China Ser. D: Earth Sci., 51, 721-729, doi, 2008.

Authors' discussion of the comments **bg_2020-312-RC2**

The authors would like to thank Reviewer #2 for his helpful comments. By taking them into consideration, the authors think that they will also clarify some of the misunderstandings of Reviewer #1.

To address the comments in the document *bg_2020-312-RC2*, the authors first copy the exact comment by the reviewer, add numbers to order each comment and make cross-referencing easier, and format in grey and Italic. The answers given by the authors are in black after each comment. In the end of the document, a list of References that support the answers was added.

General comments

The paper by Oliveira et al., provides exceptional and very valuable information about the CO_2 flux behavior immediately after a wildfire, and therefore I encourage its publication. However, the paper, in its present form is difficult to follow and should be re-structured before its publication. Results section 3.1 and 3.2 should be moved to methodology. And the section 3.3 about results should not have references. References (and its arguments) should be moved to the discussion section. See my specific comments below.

In fact, it is not easy to decide whether sections 3.1 and 3.2 should be assigned to the "methodology" section or to the "results" section, since some steps in the data processing required special analyses beyond what is standard practice. In the end, however, the authors agree to follow the arguments of Reviewer #2 to give the manuscript a clearer structure. Consequently, some results in Section 3.3 related to other sources will be included in the discussion.

The objective mentioned at the end of the introduction section is not a real objective. The "in-depth analysis of the obtained EC data" is the way (the method) to analyze the behavior of CO_2 and water vapor fluxes and its dominant factors immediately after a wildfire (your objective). Another objective of your paper could be the optimization of the quality tests for EC data to correctly interpret the obtained fluxes immediately after a wildfire.

The authors agree with revising the formulation of the objectives of the manuscript, also with regard to the notes of Reviewer #1, to emphasize the efforts for an adequate data analysis under the conditions immediately after a wildfire. The authors will take these comments of the reviewers into account in the revised version of the manuscript.

Specific comments

1. *Table 1. I think there is a mistake about the frequency of sample for net radiation. It should be 0.02Hz. This info is correctly written in the above paragraph.*

The net radiation was sampled at 20 Hz. Due to limitations in the data loggers' channels, the net radiometer had to be connected to a "fast" channel so that averaging was carried out in the same way as for "slow" data. The authors will clarify this in the final version of the manuscript.

2. *Ln 139-140 "For the cumulative fluxes over the first post-fire year, all EC data with quality classes 1-8 were combined with gap-filled data"*
   What about the footprint area? Did you also selected footprint areas that consisted for more than 80 % of the Maritime Pine stands?

The authors will clarify the text with a short remark at this point. The complete explanation is given in Section 3.3.3.

3. *Section 2.3.1. To include the % of missing half-hourly flux data due to measurement failures or rejection after the data quality check could be a very interesting information. This info can be divided into daytime and nighttime data.*

All relevant information is contained in Supplementary material Figure S8 but the authors will insert a percentage value in the manuscript.

4. *Ln 109, A parenthesis after (table 2 is missing. I would located sections 2.3.6 and 2.3.7 before section 2.3.4 because they are also related to EC measurements.*

The authors thank the reviewer for the correction regarding the parenthesis. Following the re-structuring proposed and acknowledged in the general comments, Section 2 of the final manuscript will be reorganized.

5. *Ln 223 "The test was carried out with 12,011 30-minute records that" There is something wrong in the numbers.*

The authors do not perceive what could be wrong here. A total of 17 760 records were available. For the mechanical turbulence test, 12 011 records with nearly neutral stratification were used, as specified in the sentence:

L223-L225: The test was carried out with 12,011 30-minute records that were selected for conditions of neutral stratification (-0.2 < z/L < 0.1) and data quality classes 1-8 (i.e. without footprint 225 selection).

This data selection is also shown in Figure 2 in the authors' answer to Reviewer # 1.

6. *Section 3.1 "Additional data quality test" should be section 2.4.*
7. *Section 3.1.2: Since the objective of this study is not to investigate the closure of the energy balance, I would recommend to remove this subsection and to include a sentence in section 2.3.1 with the % of the gap in the energy balance closure (that is in the range reported by most EC sites). If the authors consider that part of this subsection must appear in the manuscript, just move it into discussion section (4.1 data analisys).*
8. *The first paragraph for section 3.2.1 is "methodology" not results. Please, move this paragraph to section 2.3.2. What is more, the second paragraph is mostly discussion. Figure 7 is a result, but should be better explained in the text in order to show its relevance.*
9. *Section 3.2.2 is again "methodology" not results. Please, move this paragraph to section 2.3.2. Again, despite table 3 is a result, should be better explained in the text in order to show its relevance.*
10. *Section 3.2.3 should be also moved to "methodology" section.*

Please see answer to general comments. The authors appreciate the specific comments 6-10 and will take these in due consideration when re-structuring the manuscript.

11. *Ln 336 Please include information in the methodology section about the storage term.*

The authors will include the information about the storage term in Section 2.

12. *I would recommend to move the figure S10 into section 3.3.1. The inclusion of Figure S10 (maybe it is not necessary to include the four days) would help to the lector to better understand the Figure 8. I would*

also improve the Figure S10 (and next) including the 0 Y line for NEE and the time in the X axis. The period showed in Figure 8 can be shadow in Figure S10.

The authors agree with inserting in Figures S9 and S10 a shadow band for the 4 hours shown in Figure 8. The width is then about 6 mm. Due to the time resolution of Figures S9 and S10, very little will be visible, except for the daily cycle. The authors will show the Figures S9 and S10 in the supplement. Also, the zero line will be added

13. *The measured CO2 uptake in September and October 2017 should be due to the presence of plant cover in the studied area. Do you have some pictures to test it? Otherwise, you should provide another explanation, for the CO2 uptake in September and October 2017 (Eucalipts?).*

The authors discussed this question in detail in the answer to Reviewer #1, and also provided a orto-photomap showing the pine stands with scorched crowns and the 4 individual eucalypts. The authors will convert this discussion into additional text for the manuscript, especially elaborating on which of the possible explanations that were originally postulated (uptake by dying pine crowns or by resprouting plants, especially eucalypt) is most likely.

14. *Section 4.1. Just curiosity..., did you try to compare the cumulative NEE using your procedure for rejecting data and filling gaps and with the "standard procedure" available in https://www.bgc-jena.mpg.de/bgi/index.php/Services/REddyProcWeb?*

The processing of the measured data was carried out according to international standards (Aubinet et al. 2012) with a software package that has been compared internationally several times (Fratini and Mauder 2014). The differences in the definition of the criteria for gap-filling (data quality or u* criterion) were shown in the literature (Ruppert et al. 2006). The application of the u* criterion would result in almost 50 % of the data (instead of 10 %) having to be replaced by modelling. Therefore, there is no need to compare our results with the software package that is "standard" at the Max Planck Institute Jena (Wutzler et al. 2018), as suggested by Reviewer #1. What is certainly recommended is to compare with the software routines used in different international programs, which are standard there, just like the author (TF) did 15 years ago (Mauder et al. 2008). For such a comparison, however, the existing data set is not very suitable, since in addition to biogenic processes, chemical processes linked to the presence of wildfire ashes must also be taken into account while the observed flows were generally very small and near the detection limit.

References:

Aubinet M, Vesala T and Papale D (eds) (2012) Eddy Covariance: A Practical Guide to Measurement and Data Analysis. Springer, Dordrecht, Heidelberg, London, New York, 438 pp.

Fratini G and Mauder M (2014) Towards a consistent eddy-covariance processing: an intercomparison of EddyPro and TK3. Atmos Meas Techn. 7:2273-2281. https://doi.org/10.5194/amt-7-2273-2014

Mauder M, Foken T, Clement R, Elbers J, Eugster W, Grünwald T, Heusinkveld B and Kolle O (2008) Quality control of CarboEurope flux data - Part 2: Inter-comparison of eddy-covariance software. Biogeoscience. 5:451-462. https://doi.org/10.5194/bg-5-451-2008

Ruppert J, Mauder M, Thomas C and Lüers J (2006) Innovative gap-filling strategy for annual sums of CO_2 net ecosystem exchange. Agric For Meteorol. 138:5-18. https://doi.org/10.1016/j.agrformet.2006.03.003

Wutzler T, Lucas-Moffat A, Migliavacca M, Knauer J, Sickel K, Šigut L, Menzer O and Reichstein M (2018) Basic and extensible post-processing of eddy covariance flux data with REddyProc. Biogeosci. 15:5015-5030. https://doi.org/10.5194/bg-15-5015-2018

Reviewer #1 Reviewer #2

Estimating immediate post-fire carbon fluxes using the eddy-covariance technique

Bruna R. F. Oliveira[1], Carsten Schaller[2], J. Jacob Keizer[1], Thomas Foken[3]

[1] Earth surface processes team, Center for Environmental and Marine Studies (CESAM), Department of Environment and Planning, University of Aveiro, Aveiro, Portugal
[2] Climatology Research Group, Institute of Landscape Ecology, University of Münster, Münster, Germany
[3] Bayreuth Center of Ecology and Environmental Research (BayCEER), University of Bayreuth, Bayreuth, Germany

Correspondence to: Thomas Foken (thomas.foken@uni-bayreuth.de)

Abstract. Wildfires typically affect multiple forest ecosystem services, with carbon sequestration being affected both directly, through the combustion of vegetation, litter and soil organic matter, and indirectly, through perturbation of the energy and matter balances. Post-fire carbon fluxes continue poorly studied at the ecosystem scale, especially during the initial window-of-disturbance when changes in environmental conditions can be very pronounced due to the deposition and subsequent mobilization of a wildfire ash layer and the recovery of the vegetation. Therefore, an eddy-covariance system was installed in a burnt area as soon as possible after a wildfire that had occurred on 13 August 2017, and has been operating from the 43rd post-fire day onwards. The study site was specifically selected in a Mediterranean woodland area dominated by Maritime Pine stands with a low stature that had burnt at high severity.

The carbon fluxes recorded during the first post-fire hydrological year tended to be very low, so that a specific procedure for the analysis and, in particular, gap filling of the eddy covariance data had to be developed. Still, the carbon fluxes varied noticeably during the first post-fire year, broadly revealing five consecutive periods. During the rainless period after the wildfire, fluxes were reduced but, somewhat surprisingly, indicated a net assimilation. With the onset of the autumn rainfall, fluxes increased and corresponded to a net emission, while they became insignificant with the start of the winter. From the mid winter onwards, net fluxes became negative, indicating a weak carbon update during spring followed by a strong uptake during summer. Over the first post-fire year as a whole, the cumulative net ecosystem exchange was -347 g C m^{-2}, revealing a relatively fast recovery of the carbon sink function of the ecosystem. This recovery was mainly due to understory species, both resprouter and seeder species, since pine recruitment was reduced.

Specific periods during the first post-fire year were analyzed in detail for improving process understanding. Perhaps most surprisingly, dew formation and, more specifically, its subsequent evaporation was found to play a role in carbon emissions during the rainless period immediately after fire, involving a mechanism distinct from de-gassing of the ash/soil pores by infiltrating water. The use of a special wavelet technique was fundamental for this inference.

1 Introduction

The increasing frequency and intensity of extreme climate events (IPCC, 2018) is contributing to an increase in frequency and severity of wildfires (Flannigan et al., 2013; Keeley and Syphard, 2016). Such unprecedented wildfire regimes have been causing widespread concerns about their socio-economic and environmental impacts, including damages to ecosystems and the services they provide (Moritz et al., 2014). An important ecosystem service that is impacted by wildfires is carbon sequestration by forests (Campbell et al., 2007; Restaino and Peterson, 2013). Thereby, wildfires can interfere with forest policy and management goals for climate change mitigation (Restaino and Peterson, 2013; Ruiz-Peinado et al., 2017).

Wildfires impact forest carbon pools not only directly through combustion of vegetation and litter biomass and soil organic matter, but also indirectly through disturbance of energy, water and carbon fluxes (Sommers et al., 2014; Stevens-Rumann et al., 2017). These indirect effects are particularly difficult to assess as they depend on a complexity of factors related to fire severity, forest type, post-fire land management and post-fire environmental conditions (De la Rosa et al., 2012; Santana et al., 2016; Serrano-Ortiz et al., 2011). Furthermore, these effects can be long lasting, as illustrated by Dore et al. (2008), finding that a *Pinus ponderosa* forest was a carbon source 10-years after a stand-replacing wildfire (Supplementary Table S1).

In their review of 2013, Restaino and Peterson (2013) argued that relatively few studies had assessed post-fire carbon dynamics through the measurement of carbon fluxes as opposed to changes in carbon pools, and that relatively few of these flux studies had used the eddy-covariance (EC) technique. Marañón-Jiménez et al. (2011) likewise affirmed that post-fire studies of soil carbon effluxes were relatively abundant. To date, EC studies following wildfires continue to be scarce (Amiro, 2001; Dadi et al., 2015; Dore et al., 2008; Mkhabela et al. 2009; Serrano-Ortiz et al., 2010; Sun et al., 2016). Furthermore, only the study of Sun et al. (2016) concerned the immediate post-fire period, with EC measurements starting from the 4th month after fire. To address this knowledge gap, this study aimed to investigate carbon fluxes of Maritime Pine forest during the first hydrological year after wildfire using a flux tower, in particular after a high-severity wildfire as indicated by complete consumption of the crowns of the pine trees (following Maia et al., 2012). Because of the lack of comparable studies and because marked changes were expected in both abiotic and biotic conditions due to mobilization of wildfire ash and/or vegetation recovery, a specific objective of the present study was to get a better understanding of the different processes governing these immediate-post-fire carbon fluxes. The short study period, its dynamic conditions and the generally very small fluxes implied the need for specific, non-standard data quality tests and gap-filling procedures, especially to avoid the excessive replacement of measured fluxes by fluxes estimated with - poorly parameterized - gap-filling equations

2 Materials and Methods

2.1 Study area

The study area (N39º 37' W08º 06') was located in Vila de Rei, Portugal, in a Mediterranean climate zone at the transition of Köppen-Geiger classes Csa and Csb, with dry summers and an average temperature of 22ºC in the warmest month (Kottek et al., 2006). The study area was selected on 2 September 2017 for three main reasons: (i) having been severely affected by a recent wildfire; (ii) being dominated by Maritime Pine (*Pinus pinaster* Ait.) stands of comparatively low stature (≤10 m); (iii) consisting of relatively flat terrain within the presumed footprint area. Tree species and height were preselected based on the available, slim tower of 12 m high. The study area was a plateau of sedimentary sandstone deposits, at an elevation of 240-250 m a.s.l. (Supplementary Figure S1a), with slopes of up to 5° over an extension of approximately 10 ha (Figure 1).
The wildfire affecting the study area occurred on 13 August 2017 and burnt some 12.5 km^2 of woodland in total (ICNF, 2017). According to the European Forest Fire Information System (EFFIS, 2017), the fire severity in the study area varied between moderate and high. Fire severity was also assessed in the field, on 9 September 2017, along a 500 m transect that was laid out to the west of the slim tower, in the central part of the presumed footprint area (Supplementary Figure S1b). More specifically, severity was determined at 5 points along the transect and, at each transect point, for three plots centered on the nearest pine tree and the nearest shrub, and the inter-patch in between. At all 5 transect points, crown consumption of the pine trees exceeded 75%, undergrowth vegetation and litter were fully consumed, and wildfire ash was predominantly black. The ash layer varied in depth between 0.4 and 1.0 cm, and in cover between 55 and 100%. Soil burn severity at the 15 plots was classified according to Vega et al. (2013), and ranged from moderate-to-high (class 3) at 8 plots to high (class 4) at 7 plots.
A map of tree species in the study area was made through photo-interpretation of an ortho-photomap produced from aerial photographs that had been acquired with a RGB camera mounted on a drone (DJI Phantom 3) on 18 July 2018. Maritime Pine stands covered 90 % of the presumed footprint area, while Eucalypt (*Eucalyptus globulus*) stands occupied the remaining 10 % (Figure 2). Also, during July 2018, the pine stands in the footprint area were characterized, using 5 plots of 5 m x 5 m centered on the pine trees of the above-mentioned fire severity assessment. Median height and diameter-at-breast-height of the burnt pine trees in each of the 5 plots selected for fire severity assessment ranged from 4.6 to 6.7 m and from 2.5 to 4.3 cm, respectively. The maximum height of the trees was 7.8 m in median, ranging from 5.4 to 12.1 m in the individual plots. The densities of living pines varied from 0.24 to 1.72 trees m^{-2} before fire to 0.12 to 1.04 seedlings m^{-2} after fire. This decrease in density by the fire could be explained by the young age of the stands (in median, 12-15 years), in combination with fire damage to the (aerial) seedbank, in line with the extensive combustion of the pine crowns (Maia et al., 2012). The density of resprouting shrubs ranged from 0.0 to 0.16 shrubs m^{-2} (details on vegetation composition are given in Supplement Table S2).

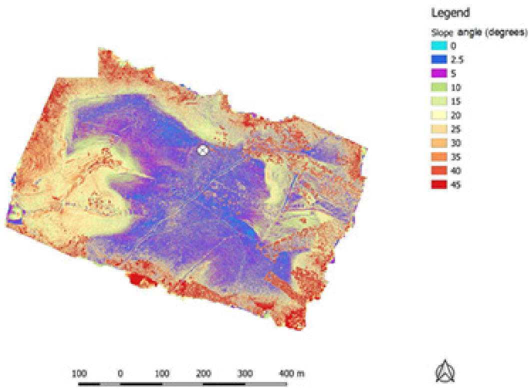

Figure 1. Slope angle map derived from aerial photography of the burnt area surrounding the flux tower. The imagery was acquired on 18 July 2028, using the standard RGB camera mounted on a DJI Phantom 3 drone.

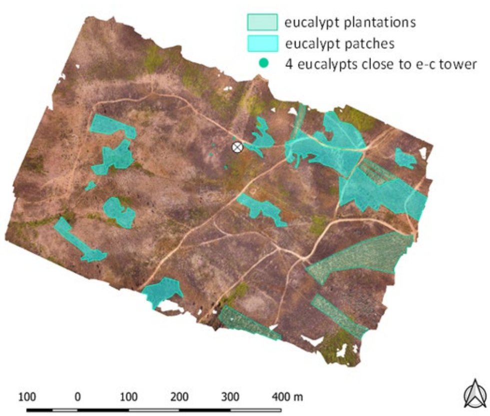

Figure 2. Ortho-photomap of the study area showing the Eucalypt stands as well as the 4 individual Eucalypt specimens close to the slim tower (cycle with cross), the rest of the area consisting of Maritime Pine stands¸ The imagery was acquired on 18 July 2018, using a standard RGB camera mounted on a DJI Phantom 3 drone.

2.2 Experimental set-up

After obtaining authorization of the land owners, the study area was instrumented with an eddy covariance system mounted on a slim tower and powered by 4 solar panels. The system was installed on 22 September 2017 and started operating four days later, i.e. 43 days after the wildfire. The exact location of the tower and the height and orientation of the gas analyzer and 3D anenometer were determined on the basis of the available regional climate information, indicating a prevalence of NW winds. This was confimed by the measurements during the first post-fire year, as shown in Figure 3.

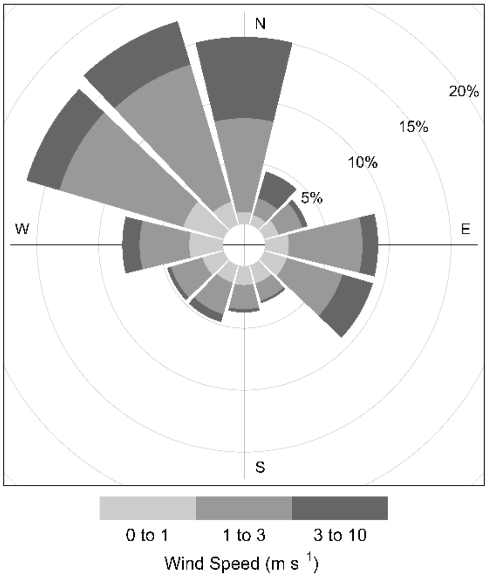

Figure 3. Wind rose of the study area over the first post-fire hydrological year (01 October 2017 – 30 September 2018), based on the sonic anemometer measurements at 11.6 m height.

A picture of the tower immediately after installation is shown in Figure 4, while the installed devices are listed in Table 1. The – standing - pine trunks in the immediate surroundings of the tower were approximately 8 m high (also in line with the above-mentioned median of 7.8 m for the maximum tree height in the presumed footprint area), and this was used as "canopy" height in all calculations, together with a zero-plane displacement of 3.8 m. The data for the calculation of the turbulent fluxes were sampled and stored at 20 Hz using a CR6 data logger from Campbell Sci. Ltd., while the fluxes were calculated over 30-minute intervals. All other data were sampled at 0.02 Hz, stored at 15-minute intervals and then averaged over the 30-minutes intervals, except for rainfall. Rainfall was recorded using two automatic rainfall gauges, with a 0.2 mm resolution and then summed over the 30-minute intervals. In addition to the soil moisture/temperature station immediately next to the tower, a soil moisture/temperature station was were installed at each of the five transect points (Supplementary Figure S1b). Each station comprised 4 EC5 soil moisture sensors and 1 GS3 soil moisture/temperature sensor. Three of a station's EC5 sensors were inserted horizontally into the soil at 2.5 cm depth, 1 immediately next to a burnt pine tree, 1 immediately next to a reprouter shrub (*Pterospartum tridentatum*), and 1 at a bare inter-patch. The 4th EC5 sensor and the GS3 sensor were also installed at the inter-patch, at a depth of 2.5 and 7.5 cm, respectively. In this study, only the data from the EC5 sensors installed at -2.5 cm depth at the 5 inter-patches were used.

This study focuses on first hydrological year after the wildfire, from 01 October 2017 to 30 September 2018. The preceding data from 26 to 30 September 2017 were only used for one of the specific cases that were analyzed in more detail to improve process understanding (Section 3.1.1).

Figure 4. The 12 m slim tower with the eddy-covariance system immediately after its installation (Photograph: J. Jacob Keizer, 22 September 2017).

Table 1. Meteorological sensors mounted on the slim tower and in its immediate surroundings.

Height	**Parameter**	**Sensor**	**Manufacturer**	**Remarks**
11.8 m	Wind vector (3 components) and sonic temperature	CSAT3	Campbell Sci Inc.	20 Hz data
11.8 m	Water vapour and carbon dioxide	LI 7500A	LiCor Biosciences	20 Hz data
1 m	Net radiation	NR lite-2	Kipp & Zonen	20 Hz data[*)]
2 m	Temperature and Relative Humidity	HMP45	Vaisala Oyj	0.02 Hz data
-2.5; -7.5; -10; -20; -30 cm	Soil temperature and volumetric water content	GS3 sensor linked to a Em50 data logger	GS3 sensor linked to a Em50 data logger	1.5 m from tower; 0.02 Hz data
-2.5; -7.5 cm	Soil volumetric water content	EC5 sensors linked to Em50 data loggers	DECAGON Devices	3 EC5 at -2.5 cm and 1 EC5 at -7.5 cm in each of 5 points along the footprint area
-2.5 cm	Soil temperature and volumetric water content	GS3 sensors linked to Em50 data loggers	DECAGON Devices	1 GS3 in 5 points along the footprint area
20 cm	Rain gauge 1 and Rain gauge 2	Tipping-bucket rain gauge with 0.2 mm resolution connected to HOBO event data logger	Pronamic (rain gauge) and Onset (data logger)	1 km to the W of tower

*) no 0.02 Hz channel was free for logging the net radiation

2.3 Eddy covariance data

2.3.1 Data calculation

The eddy covariance (EC) method is well-established to calculate energy and matter fluxes between the atmosphere and the underlying surface (Aubinet et al., 2012). Therefore, the applied procedures are only briefly described. The 30-minute EC values were calculated automatically by the Campbell EasyFlux software in the CR6 data logger but just for checking the operational status of the system. The calculations presented here were done using the software package TK3 (Mauder and Foken, 2015), which was found to compare well with other packages (Fratini and Mauder, 2014; Mauder et al., 2013). All corrections to the EC values were done following the recommendations by Foken et al. (2012), and involved spike detection, time delay correction, double rotation, and SND- and WPL-correction (Schotanus et al., 1983; Webb et al., 1980). The quality of the flux data was checked following the method by Foken and Wichura (1996) and using the latest published version of the flagging system (Foken et al., 2012). This procedure was also used in gap filling (Ruppert et al., 2006). The CO_2 storage flux is estimated by TK3 from one point CO_2 measurements, as suggested by (Hollinger et al., 1994). Finally, all 30-minute values were checked by means of an MAD analysis (Papale et al., 2006).

The footprint area was determined with the model of Kormann and Meixner (2001). More than 25 % of the EC measurements coincided with more than 80 % of the Maritime Pine stands, whereas 60 % of the measurements coincided with more than 60% of the Maritime Pine stands (Figure 5). Both percentages are high in comparison with literature (Göckede et al., 2008).

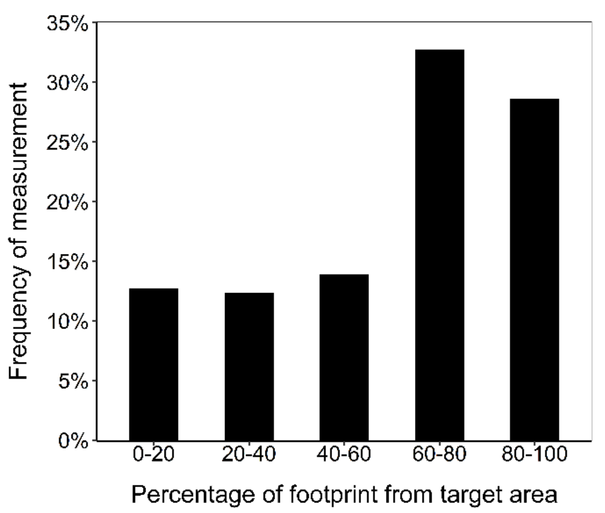

Figure 5. Distribution of the eddy covariance measurements during the first post-fire hydrological year over five classes of footprint area based on the degree of correspondence to the Maritime Pine stands.

Basic EC data analysis and, in particular, gap filling was done using the data that met quality classes 1-6 (Foken et al., 2012) and had footprint areas that consisted for more than 80 % of the Maritime Pine stands, as shown in the flow diagram of Supplementary Figure S2. The same criteria were used for selecting the specific cases presented in section 3. For the cumulative fluxes over the first post-fire year, all EC data with quality classes 1-8 were combined with gap-filled data, following the procedure shown in Supplementary Figure S3. The contribution of the eucalypt patches and trees in the footprint area to observed carbon fluxes was investigated in section 3.1.3.

2.3.2 MAD-Test

In order to eliminate some outliers (spikes) from the data selected for parameterization in the gap-filling procedure, the MAD-Test (*MAD*: Median Absolute Deviation) was applied. The MAD-Test according to Hoaglin et al. (2000), first applied to CO_2 flux data by Papale et al. (2006) and first used for de-spiking raw EC data by Mauder et al. (2013). The MAD-Test identifies as outlier all values that are outside the following range:

$$median(x) - \frac{q\,MAD}{0.6745} < x_i < median(x) + \frac{q\,MAD}{0.6745} \qquad (1)$$

where the factor of 0.6745 stems from the Gaussian distribution, and q is a threshold value that must be determined depending on the specific data set.

2.3.3 Spike test

The spike test was used in the final stage of data processing (Supplementary Figure S3). While the MAD test is used when the measured values to be examined scatter only slightly around a mean value, the spike test is used for more scattering data. This test determines the standard deviation of the entire data set and excludes all values that deviate by a multiple of the standard deviation. For the spike test, a factor of 3.5 was used as threshold, following Højstrup (1993). The spike test must be carried out multiple times until the standard deviation hardly changes, which happened after 2–4 times in this study.

2.3.4 Turbulent fluxes with high temporal resolution

The wavelet-based flux computation method was used to analyze a short-term flux event with non-steady-state fluxes during the rainless period immediately after the wildfire. This method offers the possibility to determine fluxes with a temporal resolution as high as 1 minute (Schaller et al., 2017). The wavelet method agrees well with the EC method for steady-state conditions, and was successfully applied to analyze short events of high methane fluxes in the recent studies of Göckede et al. (2019) and Schaller et al. (2019).

The wavelet method in this study applied the Mexican-hat wavelet, as it provides an excellent resolution of the fluxes in the time domain and identifies the exact moment in time when single events occur (Collineau and Brunet, 1993). The wavelet method was applied using spike-free and coordinate rotated 1-minute-data. Furthermore, the cone of influence (Torrence and Compo, 1998) was estimated to guarantee that the results were not affected by edge effects.

2.3.5. Influence of mechanical turbulence

The fact that the bulk of the burnt tree trunks continued upright during the study period raised concerns about their possible impact on turbulence conditions. Therefore, mechanical turbulence was tested according to Foken and Leclerc (2004). The test parameter is the standard deviation of the vertical wind velocity normalized by the friction velocity σ_w/u_*, and was also used here in the quality flagging of the turbulent data (Section 2.3.1). The test was carried out with 12,011 30-minute records (68 % of the data without selection of the footprint) that were selected for conditions of neutral stratification ($-0.2 < z/L < 0.1$) and data quality classes 1-8 (i.e. without footprint selection). The average and standard deviation of σ_w/u_* were 1.19 and 0.16, which agreed with available parameterizations (Foken, 2017; Panofsky et al., 1977). The data also confirmed the dependency of the test parameter on stratification (not shown here). The distribution of the test parameter according to wind direction (Figure 6) revealed higher median values for the 30-60° and 60-90° sectors. This could be explained as the typical effect of wind flowing through the tower and coming from the back side of the sonic anemometer, in line with Li et al. (2013). Furthermore, the large patch of eucalypt trees in the 30-60° sector (Figure 2) could have caused additional turbulence, especially as they re-sprouted vigorously soon after the fire. The method applied for data treatment also flagged data from these sectors. The parameter values for the other wind sectors suggested a tendency for lower median values for the sectors between 210 and 270°, and higher median values for the sectors between 270° and 30°, possibly caused by downhill and uphill flows, respectively (Figure 1). In overall terms, the values were within the typical range and did not suggest that the standing trunks of either pine or eucalypt had a relevant impact on data quality.

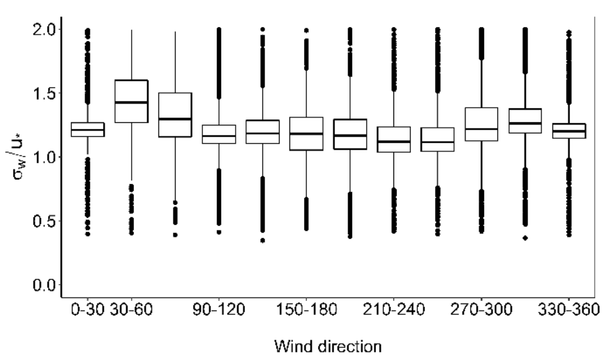

Figure 6. Box plots of the normalized standard deviation of the vertical wind velocity (σ_w/u_*) for the individual wind direction sectors.

2.3.6 Energy balance closure

The energy balance, defined as the sum of the turbulent sensible and latent heat fluxes, the net radiation and the ground heat flux, is not fully closed for many turbulent flux sites for multiple reasons that are in most cases not related to measuring errors (Foken, 2008; Mauder et al., 2020). The energy balance closure check serves to verify the general data quality of the flux measurements and should be in the usual closure gap range of < 30 % (Foken et al., 2012). In the case of the present study site, 24 June 2018 (with solar noon 12:38 UTC) was a typical example of a day with mostly clear sky, even if some influence of high clouds was suggested by the comparison of net radiation and sensible heat flux (Supplementary Figure S4). On average, there was nearly no residual; however, residuals reached values of up to 100 W m^{-2} occurred in the afternoon and even up to about 200 W m^{-2} occurred in the morning The most likely reason for these discrepancies were errors in the calculation of the ground heat flux (Section 2.5). The calculation of ground heat flux from soil temperature and volumetric moisture content may be less appropriate for post-fire condition. More specifically, the present experimental set-up ignored the presence of a – black – wildfire ash layer and may not have fully captured the soil temperature gradient. This gradient was possibly steep in the first few mm, especially when the soils were dry and still covered by wildfire ash and not yet by vegetation, due to the increased direct insolation combined with a low soil heat capacity and conductance. While the possibility that the net radiation measurements suffered from a slight inclination of the radiometer (in SW direction) cannot be altogether excluded, net radiation did appear to be underestimated. Net radiometers, as the one used in this study (Table 1), that do not measure the four up- and down-welling long- and shortwave radiation components separately, are well-known to underestimate net radiation (Kohsiek et al., 2007). In the case of the model preceding the one used in this study (i.e., the NR-lite-1), Brotzge and Duchon (2000) reported underestimations of up to 100 W m^{-2} at noon, with a strong sensitivity to the wind speed. The prevalence of negative residual fluxes during the morning was in line with an underestimation of the net radiation due to strong upwelling longwave radiation as a result of high surface temperatures, producing a bias that should be smaller during the afternoon. Because of this possible bias in the closure of the energy balance, a MAD-Test was applied to the ratio of the turbulent fluxes and the available energy (i.e. net radiation minus ground heat flux), with a factor $q = 0.5$ having been selected as optimal (Section 2.3.2). As shown in Supplementary Figure S5, the gap in energy balance closure amounted to about 10 %, which is within the range of typical values. Therefore, energy balance closure was considered not to pose a significant problem in the calculation of the fluxes.

Turbulent fluxes may also need to be corrected depending on the ratio of sensible and latent heat fluxes, i.e. the Bowen ratio. In case of a Bowen ratio larger than 1, the sensible heat flux is assumed to be underestimated; in case of a Bowen ratio below 1, both sensible and latent heat fluxes are assumed to be affected (Charuchittipan et al., 2014; Mauder et al., 2020). As shown in Supplementary Figure S6, almost all EC measurements under the driest soil conditions (VWC classes 1 and 2) had a Bowen ratio larger than 1, whereas the same was true for roughly 3 quarters of the measurements under intermediate and wet soil conditions (VWC classes 3 and 4). Therefore, the latent heat flux was not substantially affected and, hence, the CO_2 fluxes did not need further correction.

2.4. Gap-filling of respiration and assimilation

2.4.1 Basic equations

The gap-filling procedure used for substituting missing data as well as data of low quality was based on the Lloyd-Taylor and Michaelis-Menten functions, as it is a well-established procedure (Falge et al., 2001; Gu et al., 2005; Hui et al., 2004; Lasslop et al., 2010; Moffat et al., 2007; Reichstein et al., 2005).

The Lloyd-Taylor function was used to calculate respiration, Q_R:

$$Q_R = Q_{R,10} \exp\left[E_0\left(\frac{1}{283.15-T_0} - \frac{1}{T-T_0}\right)\right] \qquad (2)$$

where T is the temperature, $Q_{R,10}$ is the respiration at 10 °C, T_0 = 227.13 K and describes the temperature dependence of respiration (Falge et al., 2001; Lloyd and Taylor, 1994). The parametrization of $Q_{R,10}$ and E_0 was done using the nighttime CO_2 flux data, when assimilation is zero. The nighttime period is typically determined based on a threshold of global radiation but, since only net radiation was measured in this study, nighttime was defined here as the time window from 10 pm to 04 am UTC (UTC being the nearly local time at the study site). The parameter values were then determined using the median fluxes of 5K temperature intervals.

The parametrization of the carbon uptake at daytime, $Q_{c,\,day}$, was done with the Michaelis-Menten function (Falge et al., 2001; Michaelis and Menten, 1913), which must be determined for separate classes of temperature and global radiation:

$$Q_{c,day} = \frac{a\, R_n\, Q_{c,sat}}{a\, R_n + Q_{c,sat}} + Q_{R,day} \qquad (3)$$

where $Q_{c,sat}$ is the carbon flux at light saturation, R_n is the net radiation corrected with the longwave net radiation (as global radiation was not measured), see below, $Q_{R,\,day}$ is the respiration at daytime, and a is the linear slope of the assimilation function beginning at a global radiation of 0 W m^{-2} (Falge et al., 2001; Michaelis and Menten, 1913). The constants a and $Q_{c,sat}$ were determined by multiple regression, for separate classes of temperature and corrected net radiation.

Since global radiation was not measured in this study, assimilation was gap filled using the net radiation corrected with the longwave net radiation for an assumed cloud height of 2-4 km and assuming a low albedo of the surface, following:

$$R_{n-corr} = R_n + \sigma_{SB}[T^4 - (T-20)^4] \qquad (4)$$

where σ_{SB} is the Stefan-Boltzmann constant and T is the temperature at 11.8m height. This procedure is based on the data quality check for long-wave radiation (Gilgen et al., 1994).

2.4.2. Respiration

Standard approaches for gap filling were assumed to be less adequate for the present study for two reasons: (i) the marked recovery of the above-ground vegetation in the course of the observation period, in particular from early spring 2018 onwards; (ii) the important role of soil moisture content in soil respiration fluxes, as is typical for Mediterranean and dry ecosystems (Richardson et al., 2006; Sun et al., 2016). The latter was confirmed by a preliminary analysis of the nighttime NEE fluxes for the different soil VWC classes (not shown but evident in Figure 7), so that the gap filling was done separately for very dry to dry soil conditions (VWC classes 1 and 2), and for intermediate to wet (VWC classes 3 and 4) conditions. Respiration fluxes were determined using only the measurements from 10 pm to 04 am UTC to reduce the influence of the additive WPL correction (Webb et al., 1980), with more than 80% of the footprint area from the Maritime Pine stands, and with quality flags 1-6. The selected measurements were subsequently subjected to a MAD-Test, following Papale et al. (2006) and using $q = 0.5$ (Equation 1), The Q_{10} and E_0 parameters for the two VWC categories were estimated using the median fluxes of 5 K classes between 10 °C and 30 °C.

In the case of the (very) dry soil moisture conditions, the Q_{10} and E_0 parameters were estimated to be 0.154 µmol m^{-2} s^{-1} and 316.6, respectively. The value for Q_{10} was comparatively low (Falge et al., 2001), while E_0 was relatively high but still within the range found in other studies (Reichstein et al., 2005), comparable to that for boreal forests. In the case of the intermediate to wet soil moisture conditions, no realistic median flux values were obtained for the lowest temperature class (10 ± 2.5 °C), even if the flux data were within the detection limit and in spite of the strong data quality tests. Furthermore, the NEE data of the 12.5-17.5 °C and 17.5-22.5 °C temperature classes revealed a suspiciously strong scatter and gave rise to an unrealistically high estimate for E_0.Therefore, the abovementioned values of Q_{10} and E_0 were used for filling gaps in nighttime NEE fluxes and for estimating of daytime respiration fluxes, independent of soil moisture conditions. This most likely resulted in a underestimation of the cumulative respiration fluxes presented underneath, as Figure 7 revealed lower nighttime fluxes under very dry to dry soil moisture conditions than under intermediate to wet conditions.

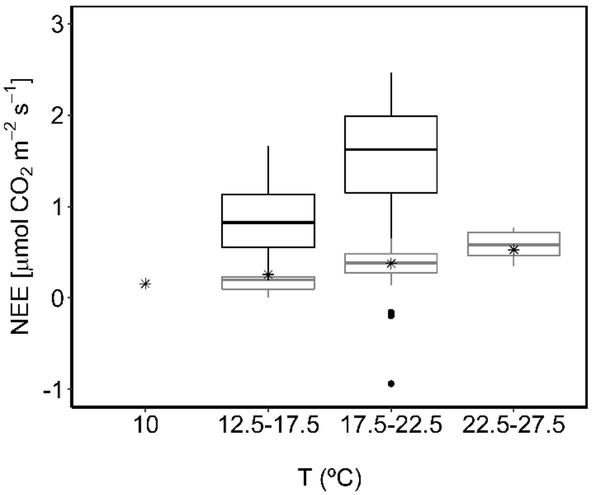

Figure 7. Box plots of the nighttime NEE fluxes for 5K temperature classes under soil moisture conditions that ranged from very dry to dry (VWC classes 1 and 2: grey boxes) and from intermediate to wet (VWC-classes 3 and 4: black boxes). The asterisks indicate the respiration fluxes calculated following the parameterization of the Lloyd-Taylor function.

2.4.3 Assimilation

According to Falge et al. (2001b) and Hollinger et al. (1994), the factor *a* in Equation 2 is the linear slope of the assimilation function beginning for a global radiation of 0 W m^{-2} and analogue for this modified net radiation. The slope of the assimilation function, *a*, and the assimilation at radiation saturation, $Q_{c,sat}$, were determined for 5 K binned classes for a data set with footprint > 80% from the pine area, and data quality classes 1-6. The results of this parameterization are summarized in Table 2.

Table 2. Values of the two constants of the Michaelis-Menten assimilation function obtained for the separate 5K classes.

Temperature	**Assimilation**	
	a	$Q_{c\ sat}$
[°C]	[µmol s^{-1} W^{-1}]	[µmol m^{-2} s^{-1}]
< 10	-0.02	-5.5
10–15	-0.02	-5.0
15–20	-0.02	-5.5
20–25	-0.02	-6.0
25–30	-0.02	-6.0
30-35	-0.02	-5.5
>35	-0.02	-5.5

2.4.4 Generation of the final data set for cumulative fluxes

The flow chart of data processing for the generation of the final data set is shown in Supplementary Figures S2 and S3. Missing data as well as data with quality flag 9, together amounting to 5% of the entire data set, were replaced with estimates computed using the Lloyd-Taylor and Michaelis-Menten functions, following the parameterizations detailed in the two prevision sections. The same was done for another 5% of the entire data set, comprising the data that did not pass the spike test that was applied to the data with quality flags 1 to 8. The nighttime period - during which assimilation was assumed zero and, hence, just the Lloyd-Taylor function was applied to estimate NEE - was defined as the time between sunset - 15 min and sunrise + 15 minutes because global radiation was not measured. Gap filling of 238 daytime 30-min records was hampered by missing net radiation data, so that they were substituted with interpolated values. The same was done for the 473 estimates from gap filling that did not pass a second spike test. For periods up to 5h, interpolated values were calculated by linear interpolation between the two values immediately before and immediately after the period; for longer periods, they were computed per time-of-the-day 30-min interval, as the average of the values of the 15 preceding and 15 succeeding days. This procedure allowed the replacement of only 10% of measured data with values estimated by gap filling. The application of a typical u_* threshold as 0.28 m s^{-1} (Wutzeler et al 2018) would have resulted in the replacement of almost 50% of the measured data. The replacement of only 10% of the data was particularly relevant due to the difficulties encountered in the parameterization of the gap-filling equations (see section 2.4), which in turn could be attributed to the short study period and its dynamic (a)biotic conditions. The present procedure did not involve a selection according to the footprint, because the CO_2 fluxes from the burned pine forest appeared to be identical to those from the burned eucalypt patches to the east of the flux tower (see section 3.1.3).

2.5 Ground heat flux

The ground heat flux was calculated from the above-mentioned soil temperature measurements (Table 1) and the heat storage of the topsoil, from the soil surface to a depth of 15 cm (Liebethal and Foken, 2007; Yang and Wang, 2008):

$$Q_G(0) = -\lambda \frac{\partial T}{\partial z}\bigg|_{z=-0.15} + \int_{-0.15}^{0} c_v(z)\, T_s\,(z)\, dz \qquad (5)$$

where T_s is the soil temperature, z is the depth, λ is the thermal molecular conductivity of the soil, and c_v is the soil's volumetric heat capacity. The accuracy of this method is comparable to that using heat flux plates (Liebethal et al., 2005). The soil temperature at 15 cm depth was calculated as the average of the temperatures at 10 and 20 cm depth, while the thermal conductivity was estimated as the mean value at the same depth, using the temperature dependent data given by Hillel (1998). The heat capacity was computed using the equation proposed by de Vries (1963), ignoring the organic soil component:

$$c_v = c_{v,m} x_m + c_{v,w} \theta \qquad (6)$$

where θ is the volumetric soil water content,, $c_{v,m}$ and $c_{v,w}$ are the heat capacities of the mineral soil compounds ($1.9 \cdot 10^6$ J m^{-3} K^{-1}) and soil water ($4.0 \cdot 10^6$ J m^{-3} K^{-1}), respectively, and x_m is the bulk density of the mineral compounds (0.566 m^3 m^{-3}), which was estimated from dry bulk density measurements of the soil and an assumed particle density of the mineral soil of 2650 kg m^{-3}.

2.6 Volumetric soil water content classes

The 30-minutes values of volumetric soil water content (VWC) of each of the 5 inter-patch sensors along the transect were first rescaled to a zero-minimum value. This was done by summing the negative minimum value over the first post-fire hydrological year (ranging from -0.07 to -0.01 m^3 m^{-3}) or, in one case, subtracting the positive minimum value (0.01). The median of the rescaled values of the 5 sensors was then calculated for each timestamp (Supplementary Figure S4). These 30-minute median values were subsequently divided, somewhat arbitrarily, into 5 classes (Table 3.

Table 3: Classes of soil volumetric water content (VWC) at 2.5 cm depth, where θ_{max} is the maximum of the 30-minute median values observed during the first hydrological year.

Class	Category	Criteria
1	Very dry	$\leq 0.1 \times \theta_{max}$
2	Dry	$> 0.1 \times \theta_{max}$ & $\leq 0.3 \times \theta_{max}$
3	Intermediate	$> 0.3 \times \theta_{max}$ & $\leq 0.7 \times \theta_{max}$
4	Wet	$> 0.7 \times \theta_{max}$ & $\leq 0.9 \times \theta_{max}$
5	Very wet	$> 0.9 \times \theta_{max}$

The temporal pattern of the 5 VWC classes during the first post-fire year is shown in Figure 8, while the corresponding pattern of the 30-minute median VWC values is given in Supplementary Figure S7. The driest soil conditions (classes 1 and 2) prevailed during the initial and final periods of this study, from October to November 2017 and from July to October 2018, while the wettest conditions (class 5) only occurred occasionally, during March 2018 following intense rainfall (see Supplementary Figure S8).

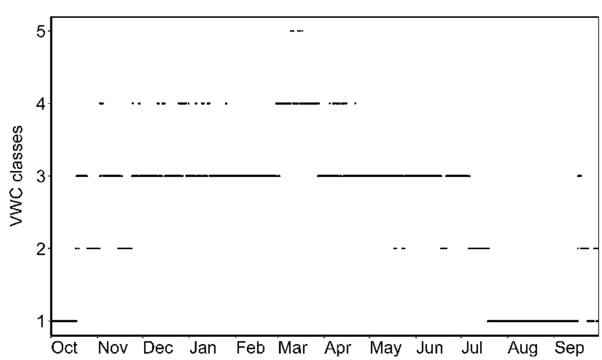

Figure 8. Volumetric water content (VWC) classes of the topsoil (from dry (1) to wet (5), as defined in Table 2) during the hydrological year 2017/18. The corresponding 30-minute VWC values are in Supplementary Figure S4.

3 Results

3.1. Selected cases

Five 3-6-day periods with good footprint conditions were selected to illustrate distinct flux conditions that were identified during the first post-fire hydrological year (including the first measurement days during September 2017).

3.1.1 The role of dew formation

The period from 26-29 September 2017, immediately after the tower became operational, was selected for revealing the role of dew formation on NEE fluxes (Supplementary Figures S9 and S10). By then, no rainfall had occurred after the wildfire (Supplementary Figure S8) and the topsoil was very dry (Figure 8). During this period, the sky was mostly clear, the sensible heat flux was of the same order as the net radiation, and the Maritime Pine stands generally comprised more than 60 % of the footprint area. The fluxes of both CO_2 and NEE (including storage term) were about zero during nighttime and showed an uptake up to -5 µmol m^{-2} s^{-1} during daytime. A substantial emission of CO_2 only occurred around sunrise on 28 September 2017, when the relative humidity at the top of the flux tower reached 80-90 % and dew formation took place. The occurrence of dew formation can be inferred from relative humidity in combination with sensible and latent heat fluxes. Dew formation simultaneously produces a positive, upward sensible heat flux due to the heat of condensation, and a negative, downward latent heat flux, while the subsequent evaporation of the dew produces fluxes of the opposite signs. Worth noting, however, is that the observed latent heat fluxes were always below the detection limit of ± 10 W m^{-2} (Mauder et al., 2006) during the early morning hours, reflecting the very dry soil conditions.

The suggestion that the positive NEE flux during the early morning of 28 September 2017 was triggered by dew formation, was further analyzed by calculating the NEE fluxes with 1-minute time resolution, using the wavelet method (Sect.2.3.4), and comparing them with the relative humidity and the sensible heat fluxes with the same time resolution (Figure 9). The WPL-correction (Webb et al., 1980) was not applied, because it would be very small under the specific conditions and, therefore, would not have noticeably changed the CO_2 fluxes.

As shown in Figure 9, relative humidity was about 80% at the top of the flux tower during the early nighttime hours of 28 September 2017, and presumably close to 100% near the ground because of the clear sky and associated temperature gradient. The recorded fluctuations in relative humidity related to fluctuations in sensible heat fluxes and CO_2 fluxes. Before 06:00 UTC, however, both fluxes were below their respective detection limits. At around 06:30 UTC, on the other hand, relative humidity increased to 85% and this increase was associated with sensible heat fluxes of up to 20 W m^{-2}, clearly in line with the occurrence of dew formation. After 07:00 UTC, relative humidity decreased again to below 80%, creating conditions for the evaporation of the dew. This dew evaporation was also indicated by negative sensible heat fluxes of up to –30 W m^{-2}

between 7.15 and 7.30 UTC, because the evaporation process requires energy. In turn, this peak in negative sensible heat fluxes was accompanied by a peak in upward CO_2 fluxes, suggesting that the upward water vapor flux worked as a kind of a pump for CO_2 emissions.

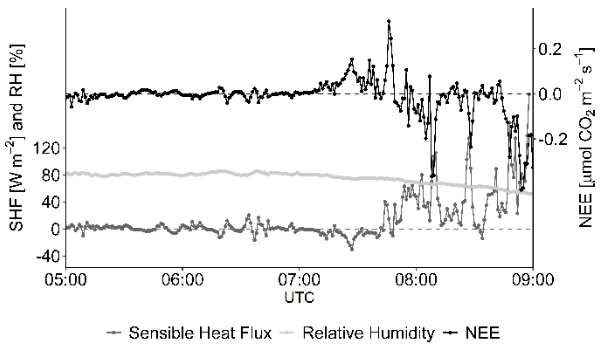

Figure 9. Relative humidity (RH) and sensible heat (SHF) and NEE fluxes with a 1-min resolution during the morning hours of 28 September 2017, indicating dew formation followed by evaporation of dew and associated CO_2 emission between 06:30 and 07:30 UTC.

3.1.2 The role of the first rainfall events after the wildfire

The first post-fire rainfall events occurred more than two months after the wildfire, between 17 to 22 October 2017 and significantly increased soil VWC (Supplementary Figures S7 and S8). The bulk of this rainfall occurred during the night from 17 to 18 October 2017 (8.4 mm) and around noon on 20 October 2017 (3.2 mm). During this 6-day period, the footprint area generally consisted for more than 80% of the Maritime Pine stands, cloudy conditions prevailed (in spite of sunny periods on 17, 18, and 22 October 2017), and the latent heat flux contributed markedly to the energy exchange (Bowen ratio of about 1; Supplementary Figure S11) because of the high relative humidity (exceeding 90% during rainfall). With the onset of the autumn rainfall, the ecosystem started to be a source of CO_2 but the fluxes decreased again on 22 October 2017. Worth noting was that the second, smaller rainfall event of 20 October 2017 seemed to have a greater impact on CO_2 emissions than the first event of 17-18 October 2017. The large scatter in NEE fluxes observed during some periods could be explained by conditions of low turbulence and the generally low fluxes.

The role of rainfall periods in NEE fluxes during the initial post-fire window-of-disturbance was also evidenced by the cumulative NEE values from 1 October to 31 December 2017 (Figure 10). After an initial period of net assimilation, three marked peaks in net CO_2 emissions occurred that were associated with periods of intense rainfall during mid-October, early and late November 2017. By contrast, intense rainfall periods during early and especially also late December 2017 only had minor impacts on net CO_2 emissions. This was probably due to the lower temperatures, ranging from 5 to 15°C during daytime.

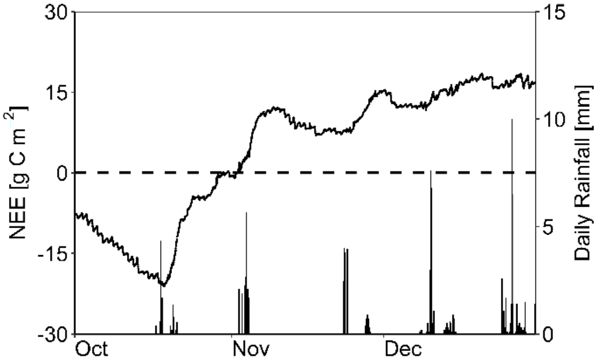

Figure 10. Cumulative NEE fluxes and 30-min rainfall during the initial window-of-disturbance, from 01 October to 31 December 2017.

3.1.3 The role of woodland type and (antecedent) rainfall during summer conditions

Energy and NEE fluxes from the Maritime Pine stands under dry conditions during the first post-fire summer are illustrated in Figure 11. During the selected, rainless 6-day period from 4 to 9 September 2018, the footprint area generally consisted for more than 80% of the pine stands, while topsoil VWC was consistently very dry (class 1; Figure 8), reflecting the less than 1 mm of antecedent rainfall over the preceding 4-week period (Supplementary Figure S8).
A second rainless summer-2018 period was selected to analyse energy and NEE fluxes from the eucalypt patches located to the east of the tower. Even though this 4-day period was about one month earlier, from 6 to 9 August 2018, topsoil VWC was equally very dry and antecedent rainfall over the preceding 4-week period was equally less than 1 mm. NEE fluxes under summer-2018 conditions did not differ conspicuously between the eucalypt (Figure 12) and Maritime Pine stands (Figure11), neither in terms of diurnal patterns nor in terms of measured values. As to be expected, sensible heat fluxes did differ markedly, being clearly higher during early August than early September. The same was true for the Bowen ratio, attaining an average value as high as 5.4 over the 6-9 August 2018 period, as opposed to 2.7 over the 4-9 September 2018 period.
A 3-day period during early July 2018 was selected to examine how summer-2018 NEE fluxes from the Maritime Pine stands (comprising > 80% of the footprint area) were affected by (antecedent) rainfall (Supplementary Figure S12). Two minor rainfall events (defined here as periods preceded and succeeded by at least 3h without rainfall) occurred on 1 July 2018. The first one started at 21.00 UTC on 30 June and ended at 02.30 UTC on 1 July and amounted to 2.0 mm, and the second lasted from 14.00 UTC to 15.30 UTC on 1 July and amounted to 0.4 mm (Supplementary Figure S8). These rainfall events lead to a minor increase in topsoil VWC (Supplementary Figure S7). Arguably, the main contrast with the early September period was the antecedent rainfall, amounting to 40,3 mm as opposed to 0.1 mm over the preceding 14 days. This contrast was also reflected in topsoil moisture conditions, which were moderate (VWC class) during early-July as opposed to very dry (VWC class 1) during early-September. The NEE fluxes during the early July-period, however, did not differ markedly from those of

the early-September period. Apparently, neither assimilation nor respiration processes suffered from serious moisture limitations by early September, in spite of the very dry conditions of the topsoil.

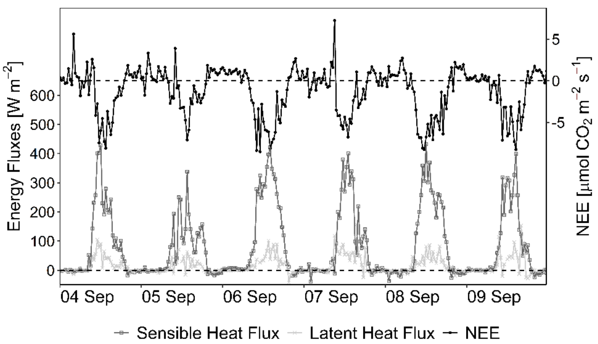

Figure 11. Energy and NEE fluxes from the Maritime Pine stands during a rainless period towards the end of the first post-fire hydrological year, from 04 to 09 September 2018.

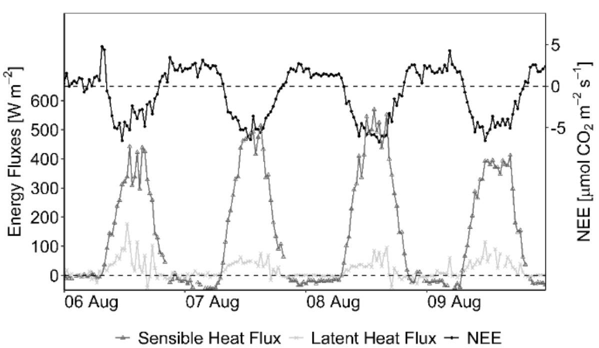

Figure 12. Daily cycles of 30-min sensible and latent heat fluxes and NEE fluxes during a rainless period in mid-summer, from 6 to 9 August 2018, when these fluxes originated from the eucalypt patches.

3.2 Cumulative Carbon dioxide fluxes

The cumulative CO_2 fluxes over the first hydrological year following the wildfire (01 October 2017 – 30 September 2018) are shown in Figure 13. No distinction was made between the fluxes from the Maritime Pine stands and those from the eucalypt stands for two reasons. First, because the pine-stand fluxes were predominant, given the prevailing WNW to N wind directions; second, because the fluxes from the two forest types appeared to be similar during summer 2018 (Section 3.1.3). In terms of NEE patterns, five different periods could be distinguished during this first post-fire year. During the immediate post-fire period, which ended with the first rainfall event on 17 October 2017, the burnt area acted as a carbon sink, even if just a small one. During the ensuing period, which ended in mid-December 2017, the burnt area functioned as a carbon source, especially following periods of intense rainfall. During the coldest period from mid-December 2017 until the end of January 2018, NEE fluxes were close to zero. With the onset of warmer temperatures during early February 2018, followed by a (practically) rainless February month, the area started to become a small carbon sink. This period continued during the next two, rainiest months, during which short intervals occurred when respiration was the dominant process. Finally, from May 2018 onwards, the area was a marked carbon sink, with assimilation clearly prevailing over respiration.

The cumulative assimilation over the first post-fire hydrological year was roughly twice the cumulative respiration. This was remarkable since forest carbon flux studies have generally found both to be of the same order of magnitude (e.g. Luyssaert et al., 2010). This discrepancy between assimilation and respiration resulted to a large extent from the last of the five above-mentioned periods, starting in May 2018. A possible reason for the discrepancy was the impossibility to parameterize respiration under intermediate and wet soil conditions and, hence, that respiration was possibly underestimated. However, the number of gap-filled data was very low.

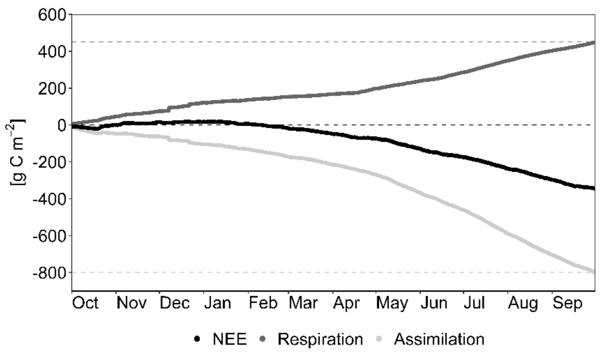

Figure 13. Cumulative NEE, assimilation and respiration fluxes during the first hydrological year after wildfire, from 01 October 2017 to 30 September 2018.

4 Discussion

The following discussion focuses on the three main novelties of this study, also because of the lack of comparable EC studies of ecosystem recovery during the initial stages following wildfire.

4.1. Data analysis

The present data set was less suited for the standard procedure of data quality assessment using a threshold of friction velocity (Goulden et al., 1996) and, hence, standardized data analysis routines as used in networks such as ICOS and NEON (Metzger et al., 2019; Rebmann et al., 2018). NEE fluxes tended to be very low during the first year after the wildfire and wind speeds were generally low, not exceeding 3 m s^{-1}. To address these particular conditions, a specific procedure was developed in the present study, based on data quality flagging (Ruppert et al., 2006). It allowed limiting the need for gap filling to about 5 % of the data, while gap filling of up to 30 % of the data is common for the fraction velocity-based procedures. The present procedure, however, required thorough data analysis, involving not only repeated MAD and spike tests and modelling of the footprint area but also assessing the possible influence of the standing burnt tree trunks on mechanical turbulence. Furthermore, an exploratory analysis of the closure of the energy balance was carried out, including because ground heat fluxes were not measured directly in this study. The energy balance closure proved acceptable, not raising major concerns about the correctness of the measured carbon fluxes. In addition, the Bowen ratio was typically in the range of 1 to 5, thereby guaranteeing that the gaps in energy balance closure did not markedly influence the carbon fluxes and that these fluxes did not require correction for such gaps (Charuchittipan et al., 2014). Gap filling itself was based on careful parameterization of the Lloyd-Taylor function, in particular by taking into account soil moisture as a key factor in the respiration of Mediterranean and dry ecosystems (Richardson et al., 2006; Sun et al., 2016). The nighttime NEE data also revealed this importance of soil moisture, but only allowed a reliable parameterization of the Lloyd-Taylor function for very dry to dry soil moisture conditions and not for intermediate to wet conditions. The latter could be due to the fact that these intermediate and wet conditions included three of the five periods that were distinguished in terms of NEE fluxes (Section 3.2), with fluxes ranging from practically zero during early winter (mid-December 2017 to end of January 2018) to their highest values during late spring (May to June 2018). Finally, the potential of the wavelet method as a complementary tool to analyse specific short-term events with an elevated temporal resolution was demonstrated, as it provided crucial insights into CO_2 fluxes during and following dew formation. The diurnal pattern in NEE fluxes was similar to the average monthly trends reported by Serrano-Ortiz et al., (2011) for a pine stand that had burnt 4 years earlier and had not been intervened afterwards. This was particularly the case for the June fluxes of Serrano-Ortiz et al., (2011) because of their greater contrast between daytime and night-time fluxes.

4.2. Respiration fluxes upon wetting by dew formation

Dew formation has been reported for many climate types, affecting, amongst others, microbial activity during rainless periods (Agam and Berliner, 2006; Gliksman et al., 2018; Verhoef et al., 2006). To the best knowledge of the authors, dew formation had not yet been observed in burnt areas. Its impact on ecosystem respiration differed fundamentally from the Birch effect that Sánchez-García et al. (2020) observed in the same burnt area as studied here and equally before the occurrence of post-fire rainfall (i.e. on 17 october 2017 in case of the site with wildfire ash). Sánchez-García et al. (2020) reported the highest soil effluxes immediately after stopping the simulated rainfall (after 10 min), but inferred, based on wetting experiments with the same soils under laboratory conditions, that peak values had occurred even earlier. The short duration of the peak was argued to suggest that the Birch effect resulted from the displacement of CO_2-rich air in soil and especially ash pores by infiltrating water (degassing), including because of the likely suppression of microbial activity due to the still recent sterilization by the fire. For the same reasons, the dew-induced CO_2 efflux observed in this study was probably due to a physical process rather than to microbial activity. This process, however, differed from the displacement of ash-soil air by infiltrating water in the sense that the respiration flux only started some half an hour after the dew formation, with the onset of the evaporation of the dew. The observed water vapor flow from the soil surface was large enough to generate a pumping effect with vertical wind velocities at the surface in the order of 10^{-4} m s^{-1} (Webb et al., 1980), on the one hand, and, on the other, the amount of dew was sufficient to explain the CO_2 efflux between 07:01 and 07.41 UTC. This CO_2 efflux amounted to 4.94 mg m^{-2} or 2.50 cm^3 m^{-2}. The sensible heat flux during this 40-min period was 17.3.10^3 J m^{-2}, i.e., involved enough energy to evaporate the 7.03 g m^{-2} or 7.02 cm^3 m^{-2} of dew, which, in turn, is equivalent to 0.41 m^3 m^{-2} of CO_2 gas (see Foken et al. (2020) for the temperature-dependent physical parameters). The occurrence of this pumping effect rather than the degassing effect observed by Sánchez-García et al. (2020) was probably due to the comparatively small amount of dew water (0.007 vs. 25 mm of simulated rain), combined with the presence of a considerable wildfire ash layer. The inter-patch ash load determined at the 5 transect points on 7 September 2017 averaged 2.21 g m^{-2}, with a minimum of 762 g m^{-2}. This ash layer will have easily absorbed the small amount of dew water, as wildfire ash has an elevated water storage capacity (Balfour and Woods, 2013; Leighton-Boyce et al., 2007). Probably, the wetting of the ash layer was limited to its immediate surface, not causing significant degassing of ash pores underneath. This wetting might have created a kind of a seal, even if perhaps a spatially heterogeneous one as Sánchez-García et al. (2020) reported that almost 50 % of the pine ash was severely to extremely water repellent. The subsequent evaporation would then have broken this seal and/or simply pumped out part of the CO_2 stored in the underlying ash pores. Further research is need to clarify to which extent the emitted CO_2 originated from a rapid restoration of microbial respiration caused by microbial biomass growth and the activation of extracellular enzymes, as has been observed after the first post-fire rainfall events (Fraser et al., 2016; Waring and Powers, 2016).

4.3. Cumulative NEE fluxes

The discussion of the cumulative NEE fluxes of this study is seriously hampered by the limited number of post-fire EC studies and, in particular, by the existence of just one prior EC study that monitored a large part of the first post-fire year (Supplementary Table S1). This latter study, of Sun et al. (2016), found that a Eucalypt spp. woodland in southern Australia was a net carbon source for a considerably longer post-fire period than the present site, i.e. until the 15^{th} instead of the 5^{th} month after fire. This delay could be due to the much drier, semi-arid climate conditions together with low soil nutrient availability, resulting in a reduced pre-fire NEP (< 100 g C m^{-2} y^{-1}) of the patchy, low-stature vegetation. The net carbon emissions during the first three monitoring months of Sun et al. (2016), however, did not differ widely from the cumulative NEE fluxes observed in this study over the 2 months following the first post-fire rainfall events (mid-October to mid-December 2017). The former ranged from 11 to 19 g C m^{-2} $month^{-1}$ for post-fire months 4 to 6, whereas the latter averaged about 20 g C m^{-2} $month^{-1}$. The other post-fire EC studies suggested that re-establishment of carbon sink function after fire took at least 1 to 9 years (Amiro et al. (2006): >1 year; Dadi et al. (2015): >2 years; Serrano-Ortiz et al. (2011): <4 years; Mkhabela et al. (2009): >6 years; Dore et al. (2008): >9 years).

Comparison of the cumulative annual NEE flux of this study with those of prior EC studies in burnt woodlands and/or unburnt pine areas (summarized in Supplementary Tables S1 and S2) showed that the present cumulative NEE of -290 g C m^{-2} y^{-1} over the first-post-fire year differed least from that reported by Moreaux et al. (2011) for their 4-year old Maritime Pine plot (-243 g C m^{-2} y^{-1}). The annual NEE of a second, intervened plot studied by Moreaux et al. (2011), however, was much lower (-65 g C m^{-2} y^{-1}). The authors attributed this to the rapid growth of shrubs and herbaceous species following the weeding and thinning, possibly even compensating a decrease in GPP by the pines due to the thinning. This intervened plot had also been studied earlier by Kowalski et al. (2003), showing that the undergrowth species started fixating carbon just a few months after the clear cutting of the original 50-year old Maritime Pine stand. Shrub species should also explain the bulk of the GPP at the present site, as their median cover at the 5 transect points by mid-September 2018 summed 50% as opposed to 3 and 2 % for herbaceous and tree species, respectively (Supplementary Table S2).

Even more unexpected than the rapid recovery of the carbon sink function at the present site was the net carbon assimilation observed during the immediate post-fire period, until the first post-fire rainfall events of mid-October 2017. The net assimilation was about 1.0 g C m^{-2} d^{-1}, i.e. between the rates during the other two periods with net assimilation (February-April 2018: 0.6 g C m^{-2} d-1; May-October 2018: 1.8 g C m-^{2} d-^{1}). Unlike the two assimilation periods from early 2018 onwards, this 2017 assimilation period was difficult to link to the recovery of the understory vegetation for two main reasons: (i) the understory vegetation was fully consumed by the fire; (ii) the recovery of the understory vegetation was still very reduced by early January, as illustrated for three key resprouter shrub species in Supplementary Figure S13. Possibly, this immediate post-fire photosynthetic activity originated from the various patches of pines with scorched crowns immediate next to the EC tower as well as at larger distance to the south and west of it, as shown in Supplementary Figure S1b. An alternative explanation would be re-sprouting eucalypts, in particular the 4 individual trees near the tower and/or the patch to the east of it, as eucalypts tend to re-sprout relatively quickly and vigorously after fire.

5. Conclusions

The main conclusion of this first study into CO_2 fluxes following wildfire over the first post-fire hydrological year were:

(i) a specific data analysis procedure including data quality flagging, MAD and spike testing, footprint analysis, soil-moisture-dependent gap filling and assessment of mechanical turbulence had to be developed because of the very low fluxes and prevailing wind speeds below 3 m s^{-1}, but allowed to reduce the need for gap filling to just about 5 % of the data;

(ii) the use of the wavelet method for the determination of turbulent fluxes with a 1-minute time resolution proved to be extremely helpful for a detailed analysis of the role of dew formation on soil respiration;

(iii) the cumulative NEE fluxes during the first hydrological year after a wildfire that occurred in August 2017 revealed an intricate temporal pattern that could be divided into five phases. The first phase (first half of October 2017) and the last two phases (from early February 2018 onwards) were (mainly) governed by assimilation, the second (mid- October to mid-December 2017) was dominated by soil respiration that was closely linked to the first post-fire rainfall events, and the third phase (mid-December 2017 to early February 2018) had negligible fluxes;

(iv) the carbon sink function of this Maritime Pine-dominated area was re-established within less than half a year after the wildfire, mainly due to the recovery of the understory vegetation of both resprouter and seeder species;
(v) dew formation during the rainless, immediate post-fire period produced a noticeable soil carbon efflux that was linked to dew evaporation and not to instantaneous degassing due to wetting.

The Supplement related to this article is available online at doi: bg-2020-312-supplement

Code and data availability. The program for the calculation of the EC data is available (Mauder and Foken, 2015). The NEE, Assimilation and Respiration data after gap-filling are available on Oliveira et al. (2020). Other data can be requested by email to bruna.oliveira@ua.pt.

Authors contribution. B.R.F. Oliveira was responsible for setting-up and operating the flux tower, carried out the analysis of the EC data, prepared the tables and figures and drafted most sections; C. Schaller carried out the wavelet analysis, analysed its results and drafted the respective section; J.J. Keizer wrote the grant proposal, coordinated the project work, created the vegetation map, analysed the soil moisture data, and drafted the respective sections; T. Foken was scientific adviser of the project, selected instrumentation of the flux tower, defined site selection criteria, outlined and supervised data analysis, conceptualized the structure of the paper and directed its write-up. All authors actively contributed and agreed with the final version of the paper.

Competing interests. The authors declare that they have no conflict of interest.

Acknowledgements. This work was supported by the project FIRE-C-BUDs (PTDC/AGR-FOR/4143/2014 - POCI-01-0145-FEDER-016780), funded by the national Foundation for Science and Technology of Portugal (FCT/MEC) with co-funding by the FEDER, within the PT2020 Partnership Agreement and Compete 2020 and with additional support by CESAM, through the strategic project UID/AMB/50017, funded by the FCT/MEC with co-funding by the FEDER, within the PT2020 Partnership Agreement and Compete 2020**.** We would like to acknowledge the help of Penelope Serrano-Ortiz from the University of Granada and the colleagues from the FIRE-C-BUDs project Isabel Campos, João Pedro Carreira (uav photography for Figures 1 and , and Supplementary Figures S2a and S2b), Mário Cerqueira, Oscar González-Pelayo, Cláudia Jesus, Paula Maia (vegetation relevees for Supplementary Table S2), Martinho Martins, Luísa Pereira, Glória Pinto, Casimiro Pio, and Alda Vieira. Furthermore, we would like to thank Nuno Costa, António Martins, José Pedro Rodrigues and Sr. Guilherme for their help in preparing and mounting the flux tower. We also thank Renato Santos, D. Benvinda and Sr. José for allowing the installation of the tower on their land.
This publication was funded by the German Research Foundation (DFG) and the University of Bayreuth within the funding program Open Access Publishing.

References

Agam, N. and Berliner, P. R.: Dew formation and water vapor adsorption in semi-arid environments - A review, J. Arid Environ., 65(4), 572–590, doi:10.1016/j.jaridenv.2005.09.004, 2006.

Amiro, B. D.: Paired-tower measurements of carbon and energy fluxes following disturbance in the boreal forest, Glob. Chang. Biol., 7(3), 253–268, doi:10.1046/j.1365-2486.2001.00398.x, 2001.

Amiro, B. D., Barr, A. G., Black, T. A., Iwashita, H., Kljun, N., McCaughey, J. H., Morgenstern, K., Murayama, S., Nesic, Z., Orchansky, A. L. and Saigusa, N.: Carbon, energy and water fluxes at mature and disturbed forest sites, Saskatchewan, Canada, Agric. For. Meteorol., 136(3–4), 237–251, doi:10.1016/j.agrformet.2004.11.012, 2006.

Aubinet, M., Vesala, T. and Papale, D. (Eds).: Eddy Covariance: A Practical Guide to Measurement and Data analysis, Springer, Dordrecht, Heidelberg, New York., 2012.

Balfour, V. N. and Woods, S. W.: The hydrological properties and the effects of hydration on vegetative ash from the Northern Rockies, USA, Catena, 111, 9–24, doi:10.1016/j.catena.2013.06.014, 2013.

Brotzge, J. A. and Duchon, C. E.: A field comparison among a domeless net radiometer, two four-component net radiometers, and a domed net radiometer, J. Atmos. Ocean. Technol., 17(12), 1569–1582, doi:10.1175/1520-0426(2000)017<1569:AFCAAD>2.0.CO;2, 2000.

Campbell, J., Donato, D., Azuma, D. and Law, B.: Pyrogenic carbon emission from a large wildfire in Oregon, United States, J. Geophys. Res. Biogeosciences, 112(4), doi:10.1029/2007JG000451, 2007.

Charuchittipan, D., Babel, W., Mauder, M., Leps, J.-P. and Foken, T.: Extension of the Averaging Time in Eddy-Covariance Measurements and Its Effect on the Energy Balance Closure, Boundary-Layer Meteorol., 152(3), 303–327, doi:10.1007/s10546-014-9922-6, 2014.

Collineau, S. and Brunet, Y.: Detection of turbulent coherent motions in a forest canopy part I: Wavelet analysis, Boundary-Layer Meteorol., 65(4), 357–379, doi:10.1007/BF00707033, 1993.

Dadi, T., Rubio, E., Martínez-García, E., López-Serrano, F. R., Andrés-Abellán, M., García-Morote, F. A. and De las Heras, J.: Post-wildfire effects on carbon and water vapour dynamics in a Spanish black pine forest., Environ. Sci. Pollut. Res. Int., 22(7), 4851–62, doi:10.1007/s11356-014-3744-4, 2015.

Dore, S., Kolb, T. E., Montes-Helu, M., Sullivan, B. W., Winslow, W. D., Hart, S. C., Kaye, J. P., Koch, G. W. and Hungate, B. A.: Long-term impact of a stand-replacing fire on ecosystem CO_2 exchange of a ponderosa pine forest, Glob. Chang. Biol., 14(8), 1801–1820, doi:10.1111/j.1365-2486.2008.01613.x, 2008.

EFFIS: COPERNICUS - Emergency Management Service. EFFIS - European Forest Fire Information System., [online] Available from: https://effis.jrc.ec.europa.eu/ (Accessed 19 September 2017), 2017.

Falge, E., Baldocchi, D., Olson, R., Anthoni, P., Aubinet, M., Bernhofer, C., Burba, G., Ceulemans, R., Clement, R., Dolman, H., Granier, A., Gross, P., Grünwald, T., Hollinger, D., Jensen, N. O., Katul, G., Keronen, P., Kowalski, A., Lai, C. T., Law, B. E., Meyers, T., Moncrieff, J., Moors, E., Munger, J. W., Pilegaard, K., Rannik, Ü., Rebmann, C., Suyker, A., Tenhunen, J., Tu, K., Verma, S., Vesala, T., Wilson, K. and Wofsy, S.: Gap filling strategies for defensible annual sums of net ecosystem exchange, Agric. For. Meteorol., 107(1), 43–69, doi:10.1016/S0168-1923(00)00225-2, 2001.

Flannigan, M., Cantin, A. S., De Groot, W. J., Wotton, M., Newbery, A. and Gowman, L. M.: Global wildland fire season severity in the 21st century, For. Ecol. Manage., 294, 54–61, doi:10.1016/j.foreco.2012.10.022, 2013.

Foken, T.: Eddy Flux Measurements the Energy Balance Closure Problem : an Overview, Ecol. Appl., 18(September), 1351–1367, doi:10.1890/06-0922.1, 2008.

Foken, T.: Micrometeorology, Second Ed., Springer Berlin Heidelberg, Berlin, Heidelberg., 2017.

Foken, T. and Leclerc, M. Y.: Methods and limitations in validation of footprint models, Agric. For. Meteorol., 127(3–4), 223–234, doi:10.1016/j.agrformet.2004.07.015, 2004.

Foken, T. and Wichura, B.: Tools for quality assessment of surface-based flux measurements, Agric. For. Meteorol., 78(1–2), 83–105, doi:10.1016/0168-1923(95)02248-1, 1996.

Foken, T., Leuning, R., Oncley, S., Mauder, M. and Aubinet, M.: Corrections and data quality, in Aubinet, M., Vesala, T. and Papale, D (Eds.) Eddy Covariance: A Practical Guide to Measurement and Data Analysis., pp. 85–131., 2012.

Foken, T., Hellmuth, O., Huwe, B. and Sonntag, D.: Physical quantities, in Handbook of Atmospheric Measurements, edited by T. Foken, Springer, Cham, in print., 2021.

Fraser, F. C., Corstanje, R., Deeks, L. K., Harris, J. A., Pawlett, M., Todman, L. C., Whitmore, A. P. and Ritz, K.: On the origin of carbon dioxide released from rewetted soils, Soil Biol. Biochem., 101, 1–5, doi:10.1016/J.SOILBIO.2016.06.032, 2016.

Fratini, G. and Mauder, M.: Towards a consistent eddy-covariance processing: An intercomparison of EddyPro and TK3, Atmos. Meas. Tech., 7(7), 2273–2281, doi:10.5194/amt-7-2273-2014, 2014.

Gilgen, H., Whitlock, C., Koch, F., Müller, G., Ohmura, A., Steiger, D. and Wheeler, R.: Technical plan for BSRN data management., 1994.

Gliksman, D., Haenel, S. and Grünzweig, J. M.: Biotic and abiotic modifications of leaf litter during dry periods affect litter mass loss and nitrogen loss during wet periods, Funct. Ecol., 32(3), 831–839, doi:10.1111/1365-2435.13018, 2018.

Göckede, M., Foken, T., Aubinet, M., Aurela, M., Banza, J., Bernhofer, C., Bonnefond, J. M., Brunet, Y., Carrara, A., Clement, R., Dellwik, E., Elbers, J., Eugster, W., Fuhrer, J., Granier, A., Grünwald, T., Heinesch, B., Janssens, I. A., Knohl, A., Koeble, R., Laurila, T., Longdoz, B., Manca, G., Marek, M., Markkanen, T., Mateus, J., Matteucci, G., Mauder, M., Migliavacca, M., Minerbi, S., Moncrieff, J., Montagnani, L., Moors, E., Ourcival, J.-M. M., Papale, D., Pereira, J., Pilegaard, K., Pita, G., Rambal, S., Rebmann, C., Rodrigues, A., Rotenberg, E., Sanz, M. J., Sedlak, P., Seufert, G., Siebicke, L., Soussana, J. F., Valentini, R., Vesala, T., Verbeeck, H. and Yakir, D.: Quality control of CarboEurope flux data - Part 1: Coupling footprint analyses with flux data quality assessment to evaluate sites in forest ecosystems, Biogeosciences, 5(2), 433–450, doi:10.5194/bg-5-433-2008, 2008.

Göckede, M., Kittler, F. and Schaller, C.: Quantifying the impact of emission outbursts and non-stationary flow on eddy-covariance CH4 flux measurements using wavelet techniques, Biogeosciences, 16(16), 3113–3131, doi:10.5194/bg-16-3113-2019, 2019.

Goulden, M. L., Munger, J. W., Fan, S.-M., Daube, B. C. and Wofsy, S. C.: Measurements of carbon sequestration by long-term eddy covariance: methods and a critical evaluation of accuracy, Glob. Chang. Biol., 2, 169–182, doi:10.1111/j.1365-2486.1996.tb00070.x, 1996.

Gu, L., Falge, E. M., Boden, T., Baldocchi, D. D., Black, T. A., Saleska, S. R., Suni, T., Verma, S., Vesala, T., Wofsy, S. C. and Xu, L.: Objective Threshold Determination for Nighttime Eddy Flux Filtering, Agric. For. Meteorol., 128, 179–197, 2005.

Hillel, D.: Environmental Soil Physics: Fundamentals, Applications, and Environmental Considerations, Academic Press, New York., 1998.

Hoaglin, D. C., Mosteller, F. and Tukey, J. W.: Understanding Robust and Exploratory Data Analysis., 2000.

Højstrup, J.: A statistical data screening procedure, Meas. Sci. Technol., 4, 153–157, 1993.

Hollinger, D. Y., Kelliher, F. M., Byers, J. N., Hunt, J. E., McSeveny, T. M. and Weir, P. L.: Carbon dioxide exchange between an undisturbed old-growth temperate forest and the atmosphere, Ecology, 75(1), 134–150, doi:10.2307/1939390, 1994.

Hui, D., Wan, S., Su, B., Katul, G., Monson, R. and Luo, Y.: Gap-filling missing data in eddy covariance measurements using multiple imputation (MI) for annual estimations, Agric. For. Meteorol., 121(1–2), 93–111, doi:10.1016/S0168-1923(03)00158-8, 2004.

ICNF: 10.º Relatório provisório de incêndios florestais - 2017. [online] Available from: http://www2.icnf.pt/portal/florestas/dfci/Resource/doc/rel/2017/10-rel-prov-1jan-31out-2017.pdf (Accessed 30 January 2019), 2017.

IPCC: Global Warming of 1.5°C. An IPCC Special Report on the impacts of global warming of 1.5°C above pre-industrial levels and related global greenhouse gas emission pathways, in the context of strengthening the global response to the threat of climate change, edited by V. Masson-Delmotte, P. Zhai, H.-O. Pörtner, D. Roberts, J. Skea, P. R. Shukla, A. Pirani, W. Moufouma-Okia, C. Péan, R. Pidcock, S. Connors, J. B. R. Matthews, Y. Chen, X. Zhou, M. I. Gomis, E. Lonnoy, T. Maycock, M. Tignor, and T. Waterfield. [online] Available from: https://report.ipcc.ch/sr15/pdf/sr15_spm_final.pdf, 2018.

Keeley, J. and Syphard, A.: Climate Change and Future Fire Regimes: Examples from California, Geosciences, 6(3), 37, doi:10.3390/geosciences6030037, 2016.

Kohsiek, W., Liebethal, C., Foken, T., Vogt, R., Oncley, S. P., Bernhofer, C. and Debruin, H. A. R.: The Energy Balance Experiment EBEX-2000. Part III: Behaviour and quality of the radiation measurements, Boundary-Layer Meteorol., 123(1), 55–75, doi:10.1007/s10546-006-9135-8, 2007.

Kormann, R. and Meixner, F. X.: An analytical footprint model for non-neutral stratification, Boundary-Layer Meteorol., 99(2), 207–224, doi:10.1023/A:1018991015119, 2001.

Kottek, M., Grieser, J., Beck, C., Rudolf, B. and Rubel, F.: World map of the Köppen-Geiger climate classification updated, Meteorol. Zeitschrift, 15(3), 259–263, doi:10.1127/0941-2948/2006/0130, 2006.

Kowalski, S., Sartore, M., Burlett, R., Berbigier, P. and Loustau, D.: The annual carbon budget of a French pine forest (Pinus pinaster) following harvest, Glob. Chang. Biol., 9(7), 1051–1065, doi:10.1046/j.1365-2486.2003.00627.x, 2003.

De la Rosa, J. M., Faria, S. R., Varela, M. E., Knicker, H., González-Vila, F. J., González-Pérez, J. A. and Keizer, J.: Characterization of wildfire effects on soil organic matter using analytical pyrolysis, Geoderma, 191, 24–30, doi:10.1016/j.geoderma.2012.01.032, 2012.

Lasslop, G., Reichstein, M., Papale, D., Richardson, A., Arneth, A., Barr, A., Stoy, P. and Wohlfahrt, G.: Separation of net ecosystem exchange into assimilation and respiration using a light response curve approach: Critical issues and global evaluation, Glob. Chang. Biol., 16(1), 187–208, doi:10.1111/j.1365-2486.2009.02041.x, 2010.

Leighton-Boyce, G., Doerr, S. H., Shakesby, R. A. and Walsh, R. P. D.: Quantifying the impact of soil water repellency on overland flow generation and erosion: a new approach using rainfall simulation and wetting agent on in situ soil, Hydrol. Process., 21, 2337–2345, doi:10.1002/hyp.6744, 2007.

Li, M., Babel, W., Tanaka, K. and Foken, T.: Note on the application of planar-fit rotation for non-omnidirectional sonic anemometers, Atmos. Meas. Tech., 6(2), 221–229, doi:10.5194/amt-6-221-2013, 2013.

Liebethal, C. and Foken, T.: Evaluation of six parameterization approaches for the ground heat flux, Theor. Appl. Climatol., 88(1–2), 43–56, doi:10.1007/s00704-005-0234-0, 2007.

Liebethal, C., Huwe, B. and Foken, T.: Sensitivity analysis for two ground heat flux calculation approaches, Agric. For. Meteorol., 132(3–4), 253–262, doi:10.1016/j.agrformet.2005.08.001, 2005.

Lloyd, J. and Taylor, J. A.: On the Temperature Dependence of Soil Respiration, Funct. Ecol., 8(3), 315–323, doi:10.2307/2389824, 1994.

Luyssaert, S., Ciais, P., Piao, S. L., Schulze, E. D., Jung, M., Zaehle, S., Schelhaas, M. J., Reichstein, M., Churkina, G., Papale, D., Abril, G., Beer, C., Grace, J., Loustau, D., Matteucci, G., Magnani, F., Nabuurs, G. J., Verbeeck, H., Sulkava, M., van der Werf, G. R. and Janssens, I. A.: The European carbon balance. Part 3: Forests, Glob. Chang. Biol., 16(5), 1429–1450, doi:10.1111/j.1365-2486.2009.02056.x, 2010.

Maia, P., Pausas, J. G., Arcenegui, V., Guerrero, C., Pérez-Bejarano, A., Mataix-Solera, J., Varela, M. E. T., Fernandes, I., Pedrosa, E. T. and Keizer, J. J.: Wildfire effects on the soil seed bank of a maritime pine stand — The importance of fire severity, Geoderma, 191, 80–88, doi:10.1016/J.GEODERMA.2012.02.001, 2012.

Marañón-Jiménez, S., Castro, J., Kowalski, A. S., Serrano-Ortiz, P., Reverter, B. R., Sánchez-Cañete, E. P. and Zamora, R.: Post-fire soil respiration in relation to burnt wood management in a Mediterranean mountain ecosystem, For. Ecol. Manage., 261(8), 1436–1447, doi:10.1016/j.foreco.2011.01.030, 2011.

Mauder, M. and Foken, T.: Eddy-Covariance software TK3, , 60, doi:10.5281/zenodo.20349, 2015.

Mauder, M., Liebethal, C., Göckede, M., Leps, J. P., Beyrich, F. and Foken, T.: Processing and quality control of flux data during LITFASS-2003, Boundary-Layer Meteorol., 121(1), 67–88, doi:10.1007/s10546-006-9094-0, 2006.

Mauder, M., Cuntz, M., Drüe, C., Graf, A., Rebmann, C., Schmid, H. P., Schmidt, M. and Steinbrecher, R.: A strategy for quality and uncertainty assessment of long-term eddy-covariance measurements, Agric. For. Meteorol., 169, 122–135, doi:10.1016/j.agrformet.2012.09.006, 2013.

Mauder, M., Foken, T. and Cuxart, J.: Surface-Energy-Balance Closure over Land: A Review, Boundary-Layer Meteorol., 177(2–3), 395–426, doi:10.1007/s10546-020-00529-6, 2020.

Metzger, S., Ayres, E., Durden, D., Florian, C., Lee, R., Lunch, C., Luo, H., Pingintha-Durden, N., Roberti, J. A., SanClements, M., Sturtevant, C., Xu, K. and Zulueta, R. C.: From NEON field sites to data portal: A community resource for surface-atmosphere research comes online, Bull. Am. Meteorol. Soc., 100(11), 2305–2325, doi:10.1175/BAMS-D-17-0307.1, 2019.

Michaelis, L. and Menten, M. L.: Die Kinetik der Invertinwirkung, Biochem. Z., 49(333–369), 1913.

Mkhabela, M. S., Amiro, B. D., Barr, A. G., Black, T. A., Hawthorne, I., Kidston, J., McCaughey, J. H., Orchansky, A. L., Nesic, Z., Sass, A., Shashkov, A. and Zha, T.: Comparison of carbon dynamics and water use efficiency following fire and harvesting in Canadian boreal forests, Agric. For. Meteorol., 149(5), 783–794, doi:10.1016/j.agrformet.2008.10.025, 2009.

Moffat, A. M., Papale, D., Reichstein, M., Hollinger, D. Y., Richardson, A. D., Barr, A. G., Beckstein, C., Braswell, B. H., Churkina, G., Desai, A. R., Falge, E., Gove, J. H., Heimann, M., Hui, D., Jarvis, A. J., Kattge, J., Noormets, A. and Stauch, V. J.: Comprehensive comparison of gap-filling techniques for eddy covariance net carbon fluxes, Agric. For. Meteorol., 147(3–4), 209–232, doi:10.1016/j.agrformet.2007.08.011, 2007.

Moreaux, V., Lamaud, É., Bosc, A., Bonnefond, J. M., Medlyn, B. E. and Loustau, D.: Paired comparison of water, energy and carbon exchanges over two young maritime pine stands (Pinus pinaster Ait.): Effects of thinning and weeding in the early stage of tree growth, Tree Physiol., 31(9), 903–921, doi:10.1093/treephys/tpr048, 2011.

Moritz, M. A., Batllori, E., Bradstock, R. A., Gill, A. M., Handmer, J., Hessburg, P. F., Leonard, J., McCaffrey, S., Odion, D. C., Schoennagel, T. and Syphard, A. D.: Learning to coexist with wildfire, Nature, 515(7525), 58–66, doi:10.1038/nature13946, 2014.

Oliveira, B. R. F., Keizer, J. J. and Foken, T.: Daily Carbon Dioxide fluxes measured by an eddy-covariance station in a recently burnt Mediterranean pine stand in Central Portugal., PANGAEA, doi:10.1594/PANGAEA.921281, 2020.

Panofsky, H. A., Tennekes, H., Lenschow, D. H. and Wyngaard, J. C.: The characteristics of turbulent velocity components in the surface layer under convective conditions, Boundary-Layer Meteorol., 11(3), 355–361, doi:10.1007/BF02186086, 1977.

Papale, D., Reichstein, M., Aubinet, M., Canfora, E., Bernhofer, C., Kutsch, W., Longdoz, B., Rambal, S., Valentini, R., Vesala, T. and Yakir, D.: Towards a standardized processing of Net Ecosystem Exchange measured with eddy covariance technique: Algorithms and uncertainty estimation, Biogeosciences, 3(4), 571–583, doi:10.5194/bg-3-571-2006, 2006.

Rebmann, C., Aubinet, M., Schmid, H., Arriga, N., Aurela, M., Burba, G., Clement, R., De Ligne, A., Fratini, G., Gielen, B., Grace, J., Graf, A., Gross, P., Haapanala, S., Herbst, M., Hörtnagl, L., Ibrom, A., Joly, L., Kljun, N., Kolle, O., Kowalski, A., Lindroth, A., Loustau, D., Mammarella, I., Mauder, M., Merbold, L., Metzger, S., Mölder, M., Montagnani, L., Papale, D., Pavelka, M., Peichl, M., Roland, M., Serrano-Ortiz, P., Siebicke, L., Steinbrecher, R., Tuovinen, J. P., Vesala, T., Wohlfahrt, G. and Franz, D.: ICOS eddy covariance flux-station site setup: A review, Int. Agrophysics, 32(4), 471–494, doi:10.1515/intag-2017-0044, 2018.

Reichstein, M., Falge, E., Baldocchi, D., Papale, D., Aubinet, M., Berbigier, P., Bernhofer, C., Buchmann, N., Gilmanov, T., Granier, A., Grünwald, T., Havránková, K., Ilvesniemi, H., Janous, D., Knohl, A., Laurila, T., Lohila, A., Loustau, D., Matteucci, G., Meyers, T., Miglietta, F., Ourcival, J. M., Pumpanen, J., Rambal, S., Rotenberg, E., Sanz, M., Tenhunen, J., Seufert, G., Vaccari, F., Vesala, T., Yakir, D. and Valentini, R.: On the separation of net ecosystem exchange into assimilation and ecosystem respiration: Review and improved algorithm, Glob. Chang. Biol., 11(9), 1424–1439, doi:10.1111/j.1365-2486.2005.001002.x, 2005.

Restaino, J. C. and Peterson, D. L.: Wildfire and fuel treatment effects on forest carbon dynamics in the western United States, For. Ecol. Manage., 303, 460–60, doi:10.1016/j.foreco.2013.03.043, 2013.

Richardson, A. D., Braswell, B. H., Hollinger, D. Y., Burman, P., Davidson, E. A., Evans, R. S., Flanagan, L. B., Munger, J. W., Savage, K., Urbanski, S. P. and Wofsy, S. C.: Comparing simple respiration models for eddy flux and dynamic chamber data, Agric. For. Meteorol., 141(2–4), 219–234, doi:10.1016/j.agrformet.2006.10.010, 2006.

Ruiz-Peinado, R., Bravo-Oviedo, A., Lopez-Senespleda, E., Bravo, F. and Rio, M.: Forest management and carbon sequestration in the Mediterranean region: A review, For. Syst., 26, eR04S, doi:10.5424/fs/2017262-11205, 2017.

Ruppert, J., Mauder, M., Thomas, C. and Lüers, J.: Innovative gap-filling strategy for annual sums of CO2 net ecosystem exchange, Agric. For. Meteorol., 138(1–4), 5–18, doi:10.1016/j.agrformet.2006.03.003, 2006.

Sánchez-García, C., Oliveira, B. R. F., Keizer, J. J., Doerr, S. H. and Urbanek, E.: Water repellency reduces soil CO2 efflux upon rewetting, Sci. Total Environ., 708, doi:10.1016/j.scitotenv.2019.135014, 2020.

Santana, V. M., González-Pelayo, O., Maia, P. A. A., Varela T., M. E., Valdecantos, A., Ramón Vallejo, V. and Jacob Keizer, J.: Effects of fire recurrence and different salvage logging techniques on carbon storage in Pinus pinaster forests from northern Portugal, Eur. J. For. Res., 135(6), 1107–1117, doi:10.1007/s10342-016-0997-0, 2016.

Schaller, C., Göckede, M. and Foken, T.: Flux calculation of short turbulent events - Comparison of three methods, Atmos. Meas. Tech., 10(3), 869–880, doi:10.5194/amt-10-869-2017, 2017.

Schaller, C., Kittler, F., Foken, T. and Göckede, M.: Characterisation of short-term extreme methane fluxes related to non-turbulent mixing above an Arctic permafrost ecosystem, Atmos. Chem. Phys., 19(6), 4041–4059, doi:10.5194/acp-19-4041-2019, 2019.

Schotanus, P., Nieuwstadt, F. T. M. and De Bruin, H. A. R.: Temperature measurement with a sonic anemometer and its application to heat and moisture fluxes, Boundary-Layer Meteorol., 26(1), 81–93, doi:10.1007/BF00164332, 1983.

Serrano-Ortiz, P., Roland, M., Sanchez-Moral, S., Janssens, I. A., Domingo, F., Goddéris, Y. and Kowalski, A. S.: Hidden, abiotic CO2 flows and gaseous reservoirs in the terrestrial carbon cycle: Review and perspectives, Agric. For. Meteorol., 150(3), 321–329, doi:10.1016/j.agrformet.2010.01.002, 2010.

Serrano-Ortiz, P., Marañón-Jiménez, S., Reverter, B. R., Sánchez-Cañete, E. P., Castro, J., Zamora, R. and Kowalski, A. S.: Post-fire salvage logging reduces carbon sequestration in Mediterranean coniferous forest, For. Ecol. Manage., 262(12), 2287–2296, doi:10.1016/j.foreco.2011.08.023, 2011.

Stevens-Rumann, C. S., Kemp, K. B., Higuera, P. E., Harvey, B. J., Rother, M. T., Donato, D. C., Morgan, P. and Veblen, T. T.: Evidence for declining forest resilience to wildfires under climate change, Ecol. Lett., doi:10.1111/ele.12889, 2017.

Sun, Q., Meyer, W. S., Koerber, G. R. and Marschner, P.: A wildfire event influences ecosystem carbon fluxes but not soil respiration in a semi-arid woodland, Agric. For. Meteorol., 226–227, 57–66, doi:10.1016/j.agrformet.2016.05.019, 2016.

Torrence, C. and Compo, G. P.: A Practical guide to wavelet analysis, Bull. Am. Meteorol. Soc., 79(1), 61–78, 1998.

Verhoef, A., Diaz-Espejo, A., Knight, J. R., Villagarcía, L. and Fernández, J. E.: Adsorption of water vapor by bare soil in an olive grove in southern Spain, J. Hydrometeorol., 7(5), 1011–1027, doi:10.1175/JHM556.1, 2006.

de Vries, D. A.: Thermal Properties of Soils, in Physics of Plant Environme, edited by W.R. van Wijk (ed), pp. 210–235, North-Holland Publishing Company, Amsterdam., 1963.

Waring, B. G. and Powers, J. S.: Unraveling the mechanisms underlying pulse dynamics of soil respiration in tropical dry forests, Environ. Res. Lett., 11(10), doi:10.1088/1748-9326/11/10/105005, 2016.

Webb, E. K., Pearman, G. I. and Leuning, R.: Correction of flux measurements for density effects due to heat and water vapour transfer, Q. J. R. Meteorol. Soc., 106(447), 85–100, doi:10.1002/qj.49710644707, 1980.

Yang, K. and Wang, J. M.: A temperature prediction-correction method for estimating surface soil heat flux from soil temperature and moisture data, Sci. China, Ser. D Earth Sci., 51(5), 721–729, doi:10.1007/s11430-008-0036-1, 2008.

Estimating immediate post-fire carbon fluxes using the eddy-covariance technique

Bruna R. F. Oliveira[1], Carsten Schaller[2], J. Jacob Keizer[1], Thomas Foken[3]

[1] Earth surface processes team, Center for Environmental and Marine Studies (CESAM), Department of Environment and Planning, University of Aveiro, Aveiro, Portugal
[2] Climatology Research Group, Institute of Landscape Ecology, University of Münster, Münster, Germany

[3] Bayreuth Center of Ecology and Environmental Research (BayCEER), University of Bayreuth, Bayreuth, Germany

Supplementary material

1. Supplementary Tables S1 to S3

Table S1. Summary of published eddy-covariance studies in woodland areas affected by wildfires

Reference	**Location**	**Climate Köppen–Geiger system**	**Dominant tree species before fire/disturbance**	**Stand observations**	**Measuring period**	**NEE** [g C m^{-2} y^{-1}]*
Present study	Central Portugal	Csb	*Pinus pinaster*	Stand replacing fire in Aug2017	Oct 2017-Oct2018	-290
Sun et al. (2016)	South Australia	Bsk	*Eucalyptus dumosa, E incrassata, E oleosa, E socialis*	1-y after fire May2014-Jul2015	May14	19 g C m^{-2} $month^{-1}$
					Jun14	16 g C m^{-2} $month^{-1}$
					Jul14	11 g C m^{-2} $month^{-1}$
					May15	-18 g C m^{-2} $month^{-1}$
					Jun15	-13 g C m^{-2} $month^{-1}$
					Jul15	-12 g C m^{-2} $month^{-1}$
Dadi et al. (2015)	Cuenca, Spain	Csb	*Pinus nigra*	High severity, stand-replacing fire in July 2009	Jun2011-Feb2013	180
Serrano-Ortiz et al. (2011)	SE Spain	Dsc	*Pinus sylvestris*	Burnt Sept 2005; Salvage logging (SL) vs no intervention (NI)	Jun-Dec 2009	BUR-SL 40 g C m^{-2} per 7-months
						BUR-NI -90 g C m^{-2} per 7-months
Mkhabela et al. (2009)	Saskatchewan, Canada	Dfb	*Pinus banksiana*	BUR 1998	2004 and 2005	20
				BUR 1989		-84

				BUR 1977		+58
				BUR 1929		-20
Dore et al. (2008)	Arizona, USA	Csa	*Pinus ponderosa*	High severity, stand-replacing fire 1996 vs Unburnt	Sep 2005 to Dec 2006	109±6
Amiro (2001)	NW Canada	Dfc	*Pinus banksiana*	Severely burnt in July 1997; Adjacent UNB with 80 years	7-15 Jul 1998	BUR 0.8 g C m^{-2} d^{-1}
				Burnt 1989 and aerially seeded in 1990; Adjacent UNB with 50 years	10-26 Aug1999	BUR = UNB -1.3 g C m^{-2} d^{-1}

*unless other units indicated

Table S2. Summary of the floristic composition on 10 September 2018 as determined by vegetation relevees at the 5 points along the transect in the targeted footprint area

Higher plant species	Projected ground cover ((minimum) median (maximum)%)
Cistus psilosepalus	(0) 0 (40)
Agrostis truncatula	(0) 0 (15)
Cistus ladanifer	(1) 15 (30)
Eucalyptus globulus	(0) 0 (10)
Halimium ocymoides	(0) 9 (15)
Calluna vulgaris	(0) 1 (15)
Pterospartum tridentatum	(0) 5 (10)
Erica spec.	(0) 0 (5)
Arbutus unedo	(0) 0 (5)
Phyllirea angustifolia	(0) 1 (10)
Pinus pinaster	(1) 2 (5)
Lavandula pedunculata	(0) 0 (2)
Genista triachantos	(0) 1 (2)
Conyza bonariensis	(0) 0 (2)
Anarrhinum bellidifolium	(0) 0 (1)
Pteridium aquilinum	(0) 0 (1)
Jasione montana	(0) 0 (1)
Hakea sericea	(0) 0 (1)
Ornithopus spec.	(0) 1 (1)

Table S2. Summary of published eddy-covariance studies in unburnt *Pinus pinaster Ait.* woodlands

Reference	**Location**	**Climate**	**Dominant tree species**	**Soil**	**Stand establishment**	**Tree age** [y]	**NEP** [g C m^{-2} y^{-1}]*
Berbigier et al. (2001)	Bordeaux, France	Cfb	*Pinus pinaster Ait*	sandy hydromorphic podzol	Planted in 1970	28	575
Kowalski et al. (2003)	Les Landes, France	Cfb	*Pinus pinaster Ait.*	sandy podzol	Clear-felled 50 y old plantation	1	-290
Jarosz et al. (2008)	Bordeaux, France	Cfb	*Pinus pinaster Ait.*	Sandy hydromorphic podzol	Planted in 1970	32	79 total -59 understory 138 tree layer
Moreaux et al. (2011)	Bordeaus, France	Cfb	*Pinus pinaster Ait.*	Sandy podzol	Clear cut 1999; ploughed and fertilized 2001; seeded 2004. A: without intervention B: removal of weed and thinning of trees in 2008/2009	A: 4 B: 5	243 65
Matteucci et al. (2015)	Tuscany, Italy	Csa (study year was atypically dry)	*Pinus pinaster Ait.*	93% sand, 3% silt; 4% clay. 43.8% SOM	Natural regeneration following a wildfire in 1944	64	(May'01-March'02) 21

*unless other units indicate

2. Supplementary Figures S1 to S13

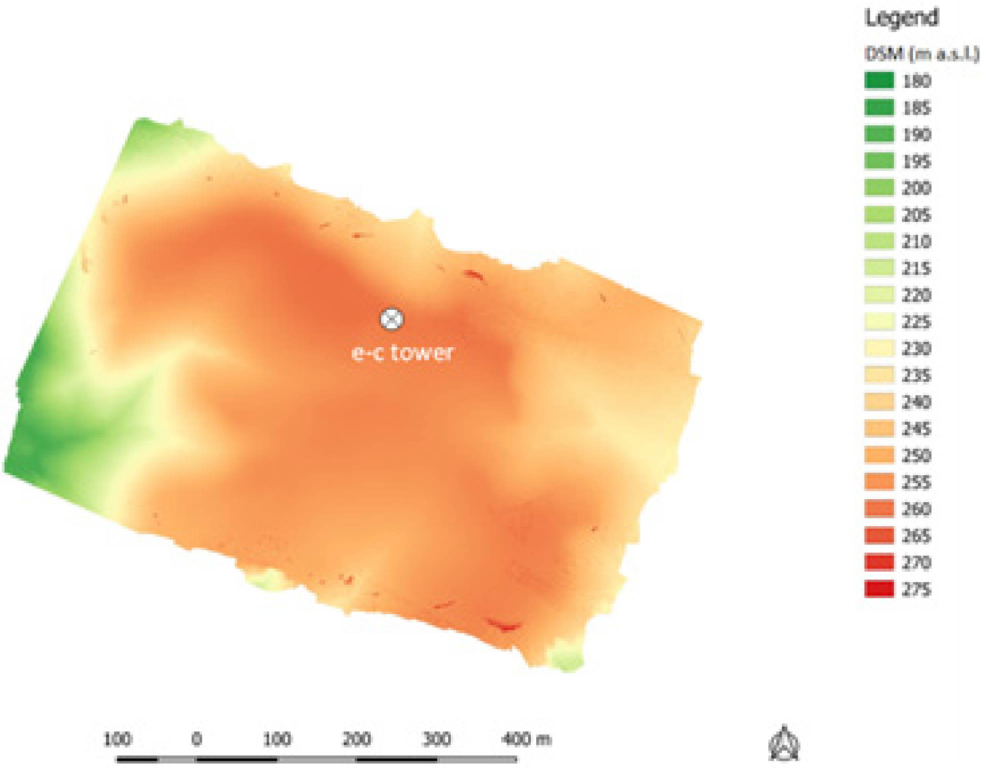

Figure S1a. Digital surface model derived from aerial photography of the burnt area surrounding the flux tower (marked with a circle with a cross). The imagery was acquired on 18 July 2018, using the standard RGB camera mounted on a DJI Phantom 3 drone.

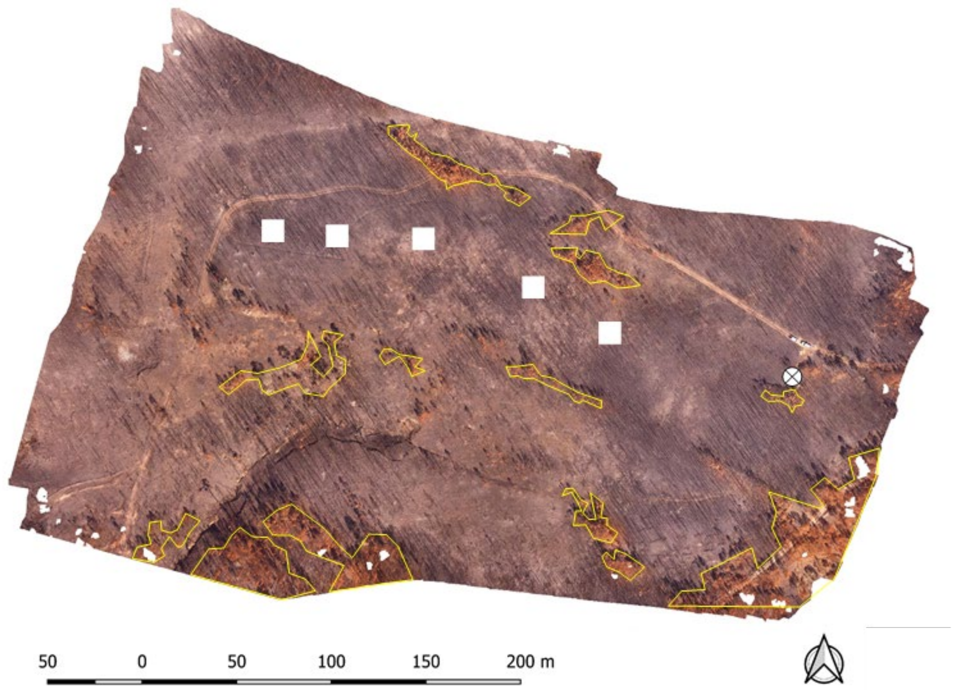

Figure S1b. Ortho-photomap of the study area showing the patches of pine trees whose crowns were only scorched by the wildfire (yellow-bounded polygons), and the 5 points (white squares) along the transect laid out the west of slim tower (cycle with cross), The imagery was acquired roughly 6 weeks after the wildfire, on 22 September 2017, using a standard RGB camera mounted on a DJI Phantom 3 drone

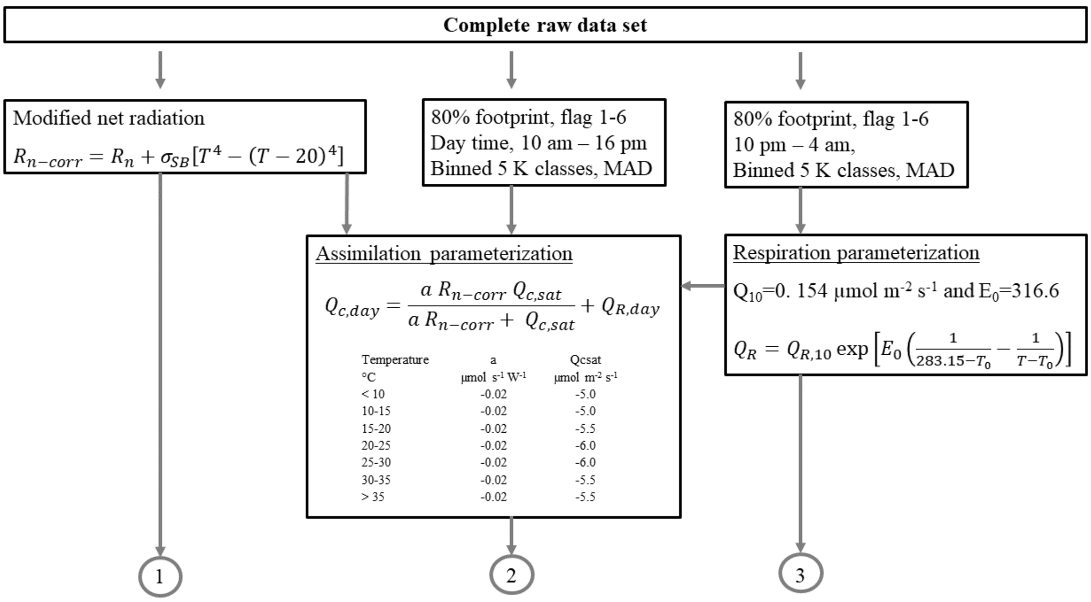

Figure S2. Flow chart of the calculation of the parameters for gap filling of 30-min assimilation and respiration fluxes.

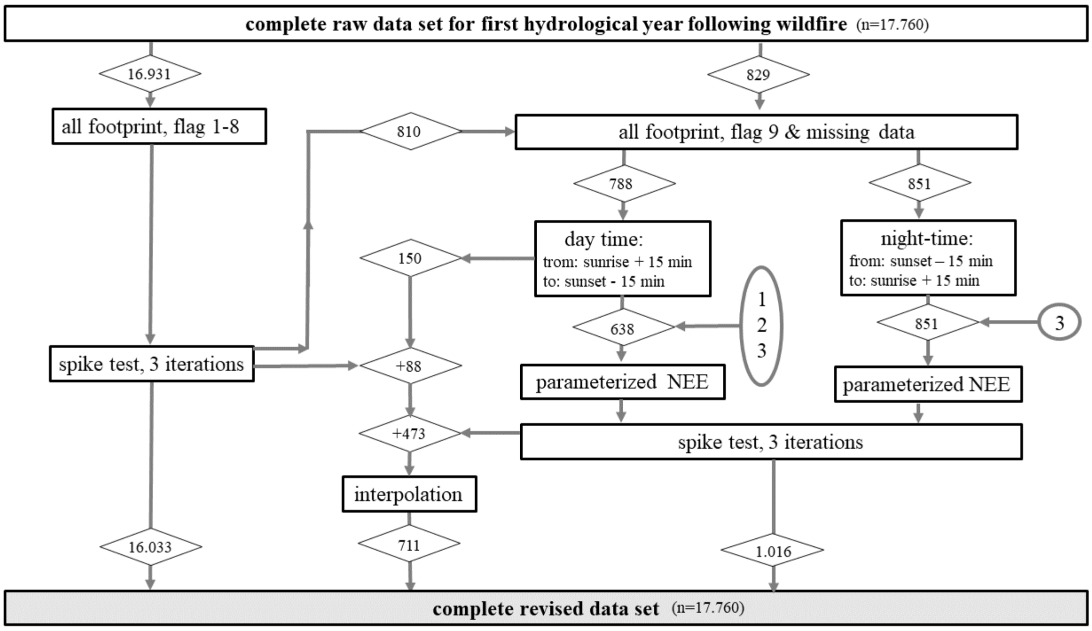

Figure S3. Flow chart of the revision of the raw 30-min data.

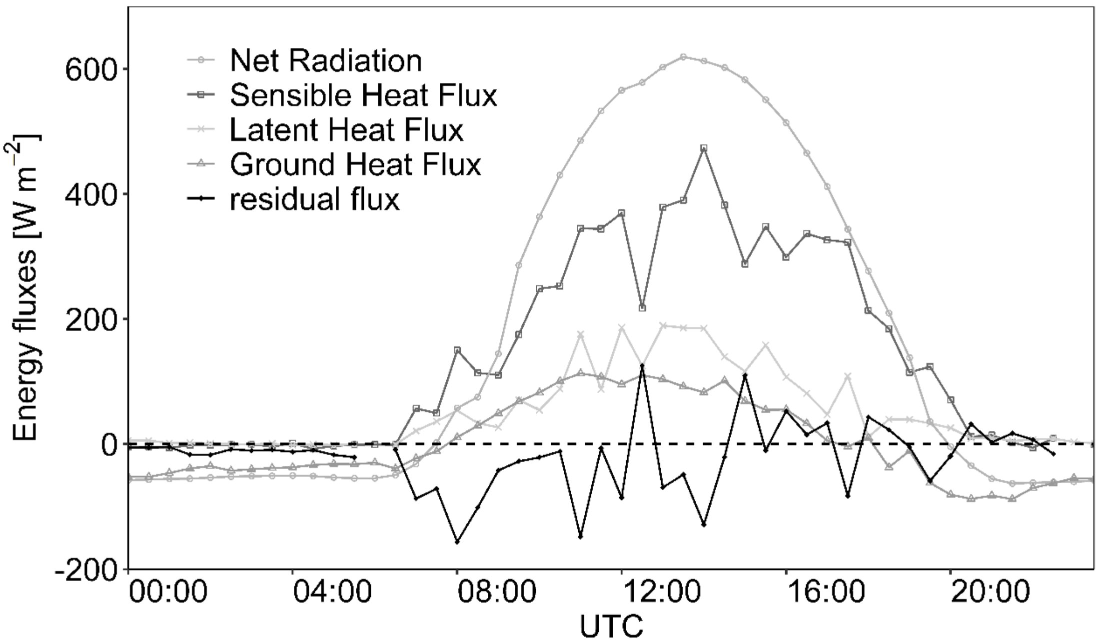

Figure S4. Daily cycle of energy fluxes and their residual on 24 June 2018, when the sky was predominantly clear, except for some high clouds around the local noon at 12:38 UTC. From 08:00 to 19:30 UTC, the footprint consisted for more than 80% of the Maritime pine woodland.

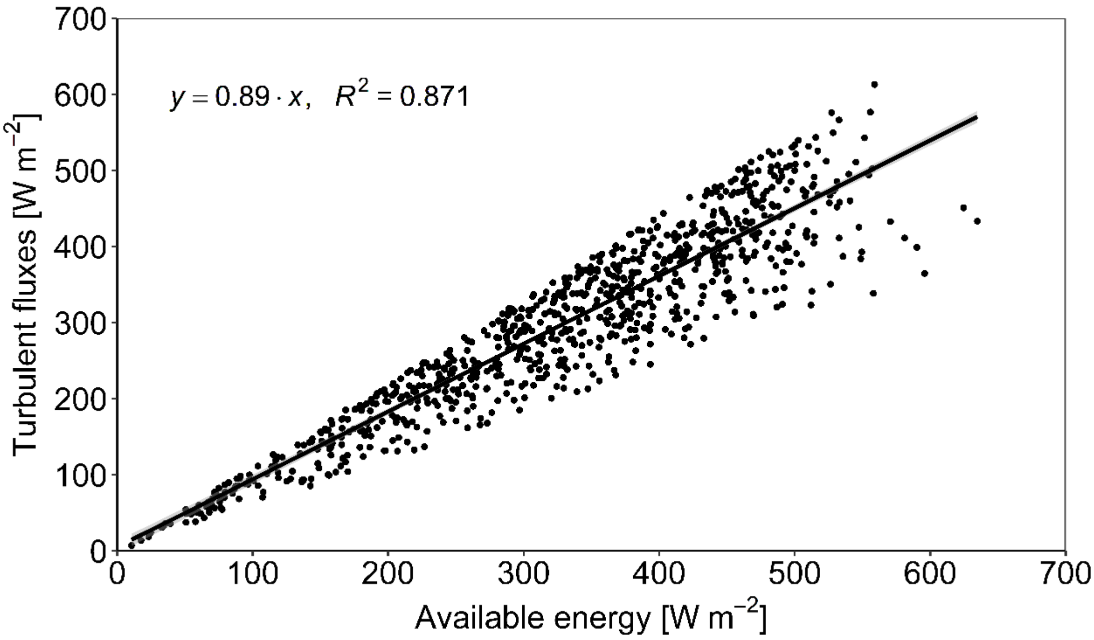

Figure S5. Relationship of turbulent fluxes with available energy for all 30-minute data records that met four conditions: (i) >80% of the footprint area corresponded to the burnt pine woodland; (ii) the quality flags for the turbulent fluxes ranged from 1 to 6; (iii) sensible and latent heat fluxes were larger than the detection limit of 10 W m^{-2}; the ration of latent to sensible heat fluxes passed a MAD-test with q=0.5.

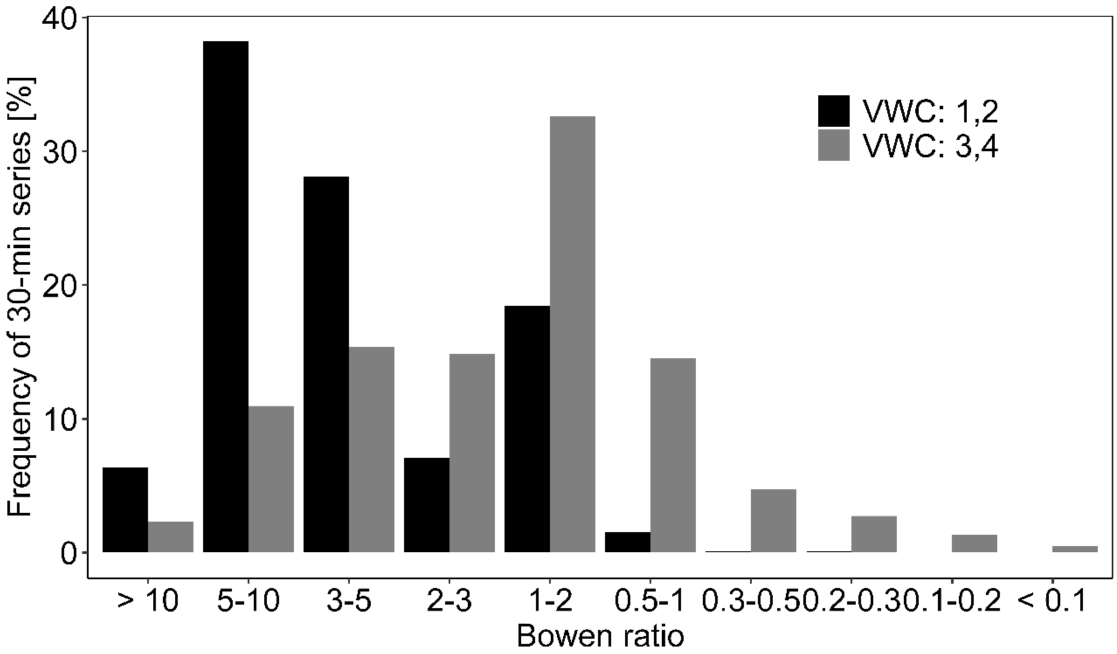

Figure S6. Frequency distribution of the ratio of sensible and latent heat fluxes (Bowen ratio) for two contrasting soil moisture conditions (Volumetric Water Content classes 1 and 2 vs. 3 and 4). The same 30-minute data records as used for Figure S5.

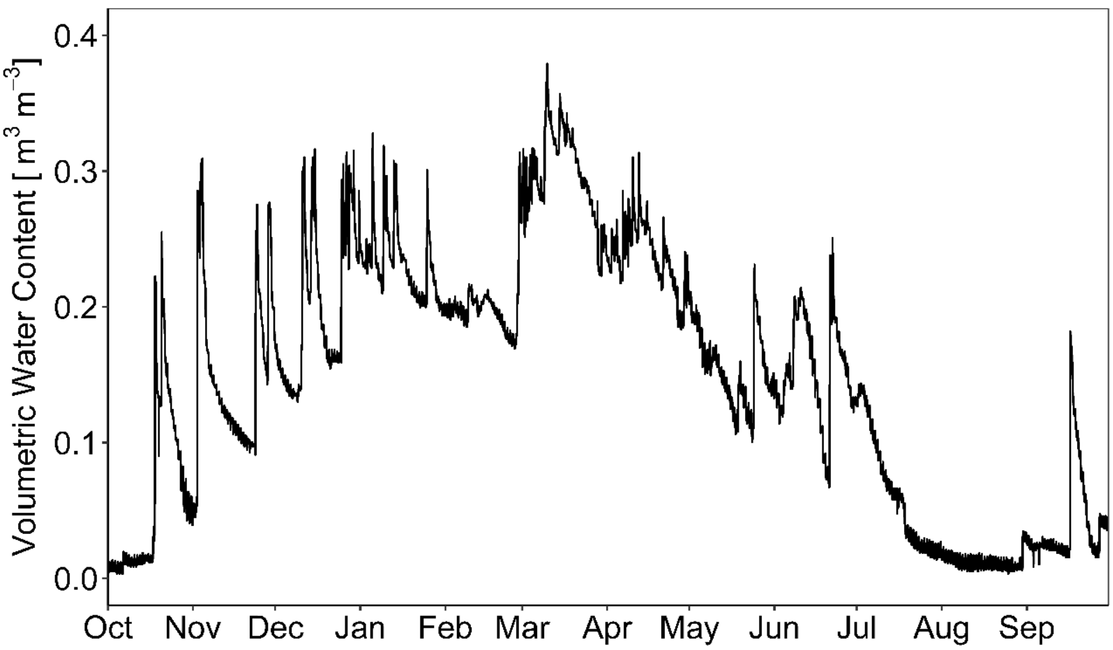

Figure S7. Median 30- minute volumetric soil water content during the 2017/18 hydrological year at 2.5 cm depth at five inter-patches along a transect laid out to the west of the flux tower in the Maritime pine footprint area.

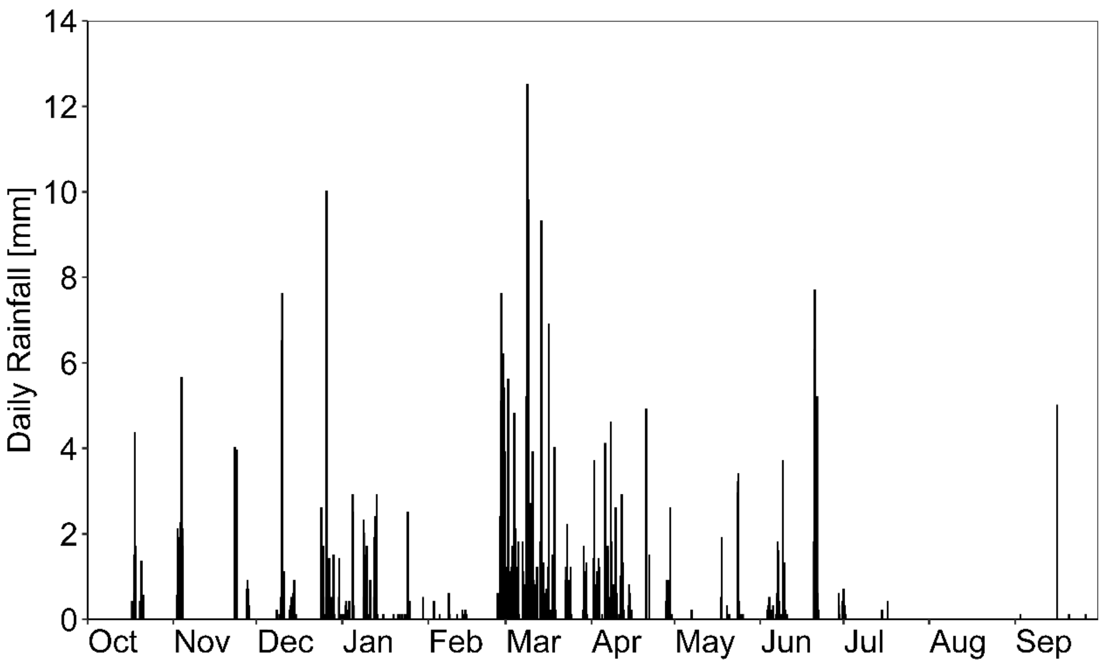

Figure S8: Daily rainfall during the 2017/18 hydrological year as recorded by the automatic gauges installed in the study area.

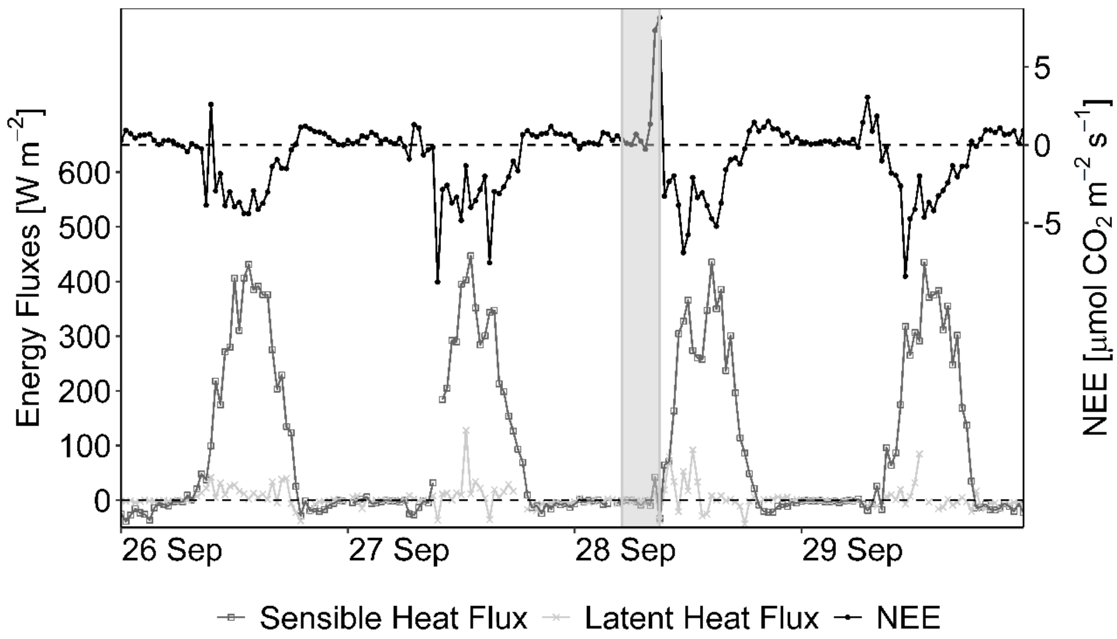

Figure S9. Daily cycles of 30-min sensible and latent heat fluxes and NEE fluxes for the immediate post-fire period from 26 to 29 September 2017. Figure S10 shows the daily cycles of relative humidity together with those of the NEE fluxes. The shadow band shows the time interval of Figure 9.

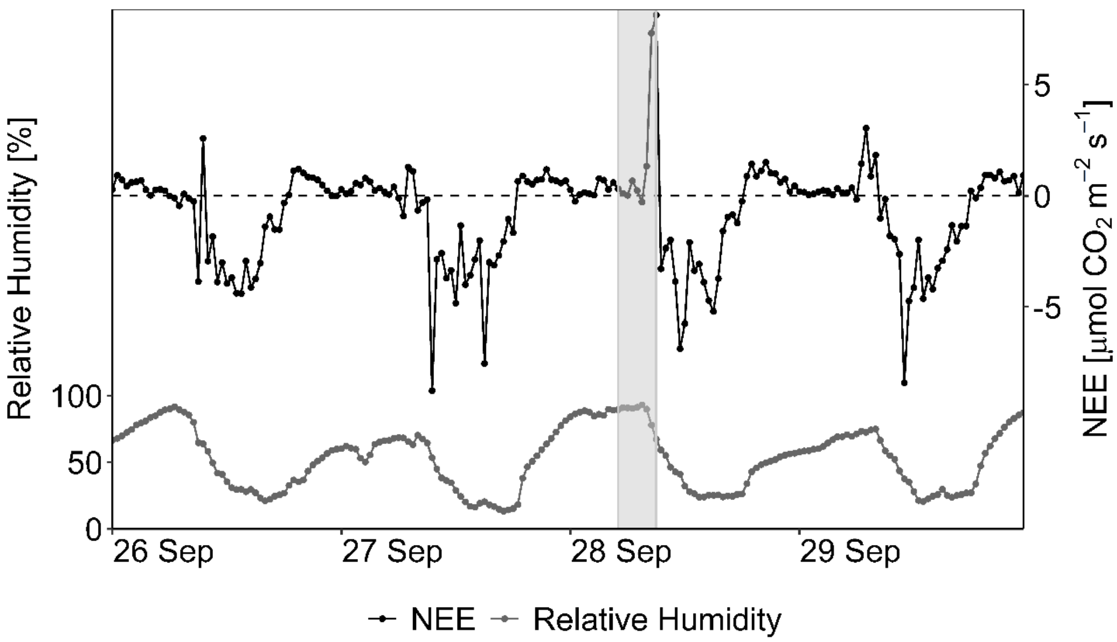

Figure S10. Daily cycles of 30-min relative humidity and NEE fluxes for the immediate post-fire period from 26 to 29 September 2017. The shadow band shows the time interval of Figure 9.

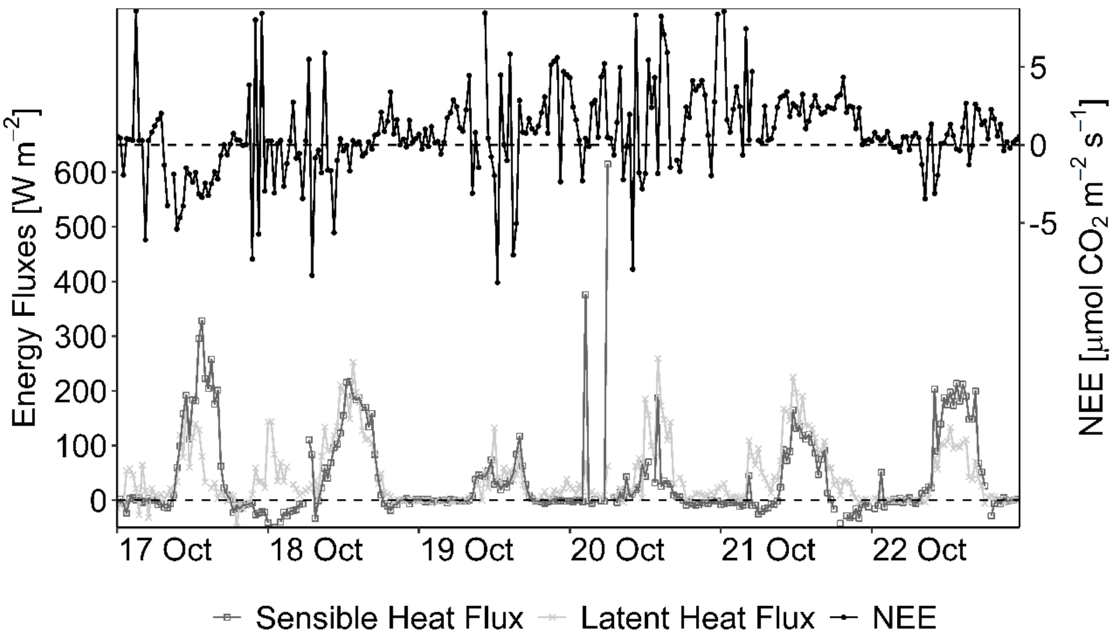

Figure S11. Daily cycles of 30-min sensible and latent heat fluxes and NEE fluxes following the first two significant post-fire rainfall events during the night from 17 to 18 October 2017 and around noon on 20 October 2017.

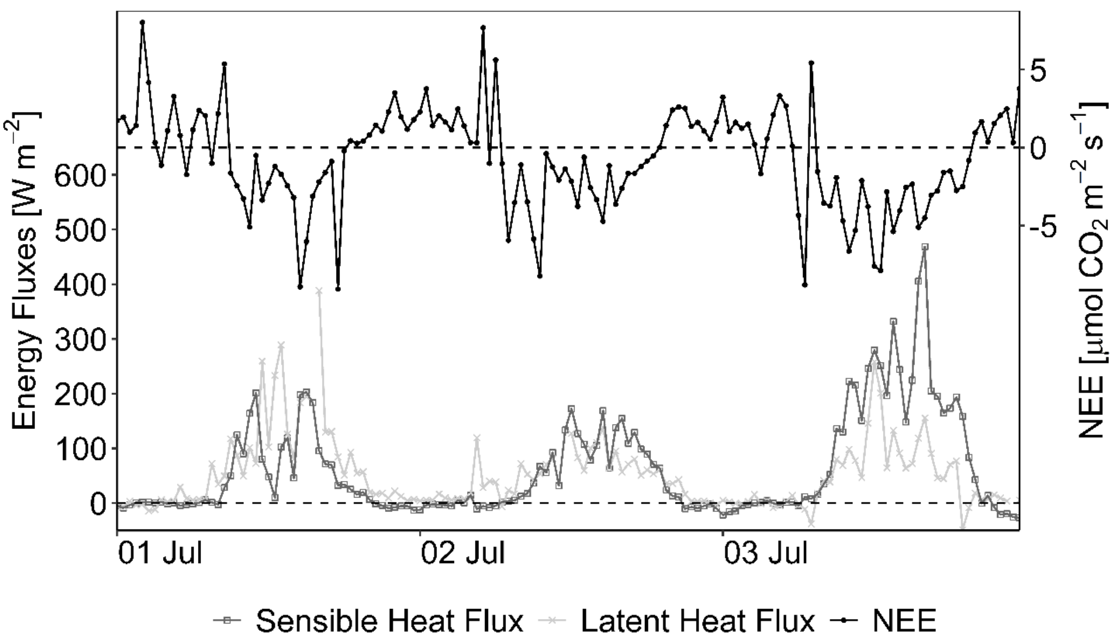

Figure S12. Daily cycles of 30-min sensible and latent heat fluxes and NEE fluxes during early summer 2018, from 1 to 3 July, when these fluxes originated from the Maritime pine woodlands.

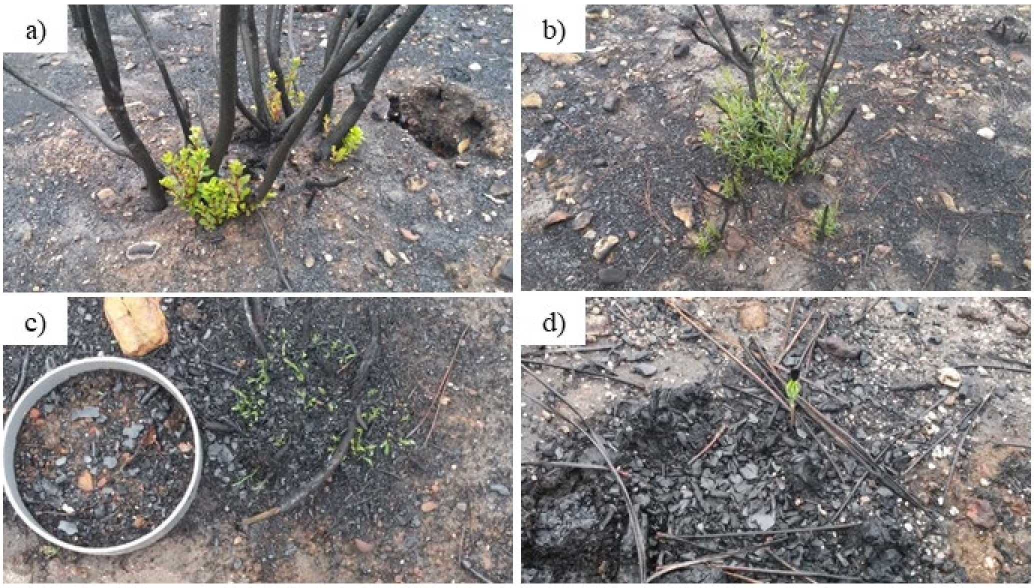

Figure S13. Illustration of post-fire vegetation recovery by 3 January 2018, showing three resprouter shrub species of the understory (a) *Arbutus unedo*; b) *Phillyrea angustifolia*; c) *Pterospartum tridentatum*; and d) Maritime pine seedling. (Pictures by J. Jacob Keizer)

References

Amiro, B. D.: Paired-tower measurements of carbon and energy fluxes following disturbance in the boreal forest, Glob. Chang. Biol., 7(3), 253–268, doi:10.1046/j.1365-2486.2001.00398.x, 2001.

Berbigier, P., Bonnefond, J.-M. M. and Mellmann, P.: CO2 and water vapour fluxes for 2 years above Euroflux forest site, Agric. For. Meteorol., 108(3), 183–197, doi:10.1016/S0168-1923(01)00240-4, 2001.

Chan, F. C. C., Altaf Arain, M., Khomik, M., Brodeur, J. J., Peichl, M., Restrepo-Coupe, N., Thorne, R., Beamesderfer, E., McKenzie, S., Xu, B., Croft, H., Pejam, M., Trant, J., Kula, M. and Skubel, R.: Carbon, water and energy exchange dynamics of a young pine plantation forest during the initial fourteen years of growth, For. Ecol. Manage., 410, 12–26, doi:10.1016/J.FORECO.2017.12.024, 2018.

Dadi, T., Rubio, E., Martínez-García, E., López-Serrano, F. R., Andrés-Abellán, M., García-Morote, F. A. and De las Heras, J.: Post-wildfire effects on carbon and water vapour dynamics in a Spanish black pine forest., Environ. Sci. Pollut. Res. Int., 22(7), 4851–62, doi:10.1007/s11356-014-3744-4, 2015.

Dore, S., Kolb, T. E., Montes-Helu, M., Sullivan, B. W., Winslow, W. D., Hart, S. C., Kaye, J. P., Koch, G. W. and Hungate, B. A.: Long-term impact of a stand-replacing fire on ecosystem CO2 exchange of a ponderosa pine forest, Glob. Chang. Biol., 14(8), 1801–1820, doi:10.1111/j.1365-2486.2008.01613.x, 2008.

van Gorsel, E., Berni, J. A. J., Briggs, P., Cabello-Leblic, A., Chasmer, L., Cleugh, H. A., Hacker, J., Hantson, S., Haverd, V., Hughes, D., Hopkinson, C., Keith, H., Kljun, N., Leuning, R., Yebra, M. and Zegelin, S.: Primary and secondary effects of climate variability on net ecosystem carbon exchange in an evergreen Eucalyptus forest, Agric. For. Meteorol., 182–183, 248–256, doi:10.1016/J.AGRFORMET.2013.04.027, 2013.

Jarosz, N., Brunet, Y., Lamaud, E., Irvine, M., Bonnefond, J.-M. and Loustau, D.: Carbon dioxide and energy flux partitioning between the understorey and the overstorey of a maritime pine forest during a year with reduced soil water availability, Agric. For. Meteorol., 148(10), 1508–1523, doi:10.1016/J.AGRFORMET.2008.05.001, 2008.

Kowalski, S., Sartore, M., Burlett, R., Berbigier, P. and Loustau, D.: The annual carbon budget of a French pine forest (Pinus pinaster) following harvest, Glob. Chang. Biol., 9(7), 1051–1065, doi:10.1046/j.1365-2486.2003.00627.x, 2003.

Kulmala, L., Pumpanen, J., Kolari, P., Dengel, S., Berninger, F., Köster, K., Matkala, L., Vanhatalo, A., Vesala, T. and Bäck, J.: Inter- and intra-annual dynamics of photosynthesis differ between forest floor vegetation and tree canopy in a subarctic Scots pine stand, Agric. For. Meteorol., 271, 1–11, doi:10.1016/J.AGRFORMET.2019.02.029, 2019.

Matteucci, M., Gruening, C., Goded Ballarin, I., Seufert, G. and Cescatti, A.: Components, drivers and temporal dynamics of ecosystem respiration in a Mediterranean pine forest, Soil Biol. Biochem., 88, 224–235, doi:10.1016/j.soilbio.2015.05.017, 2015.

Mkhabela, M. S., Amiro, B. D., Barr, A. G., Black, T. A., Hawthorne, I., Kidston, J., McCaughey, J. H., Orchansky, A. L., Nesic, Z., Sass, A., Shashkov, A. and Zha, T.: Comparison of carbon dynamics and water use efficiency following fire and harvesting in Canadian boreal forests, Agric. For. Meteorol., 149(5), 783–794, doi:10.1016/j.agrformet.2008.10.025, 2009.

Moreaux, V., Lamaud, É., Bosc, A., Bonnefond, J. M., Medlyn, B. E. and Loustau, D.: Paired comparison of water, energy and carbon exchanges over two young maritime pine stands (Pinus pinaster Ait.): Effects of thinning and weeding in the early stage of tree growth, Tree Physiol., 31(9), 903–921, doi:10.1093/treephys/tpr048, 2011.

Peichl, M., Brodeur, J. J., Khomik, M. and Arain, M. A.: Biometric and eddy-covariance based estimates of carbon fluxes in an age-sequence of temperate pine forests, Agric. For. Meteorol., 150(7–8), 952–965, doi:10.1016/J.AGRFORMET.2010.03.002, 2010.

Rodrigues, A., Pita, G., Mateus, J., Kurz-Besson, C., Casquilho, M., Cerasoli, S., Gomes, A. and Pereira, J.: Eight years of continuous carbon fluxes measurements in a Portuguese eucalypt stand under two main events: Drought and felling, Agric. For. Meteorol., 151(4), 493–507, doi:10.1016/J.AGRFORMET.2010.12.007, 2011.

Serrano-Ortiz, P., Marañón-Jiménez, S., Reverter, B. R., Sánchez-Cañete, E. P., Castro, J., Zamora, R. and Kowalski, A. S.: Post-fire salvage logging reduces carbon sequestration in Mediterranean coniferous forest, For. Ecol. Manage., 262(12), 2287–2296, doi:10.1016/j.foreco.2011.08.023, 2011.

Sun, Q., Meyer, W. S., Koerber, G. R. and Marschner, P.: A wildfire event influences ecosystem carbon fluxes but not soil respiration in a semi-arid woodland, Agric. For. Meteorol., 226–227, 57–66, doi:10.1016/j.agrformet.2016.05.019, 2016.